EPITHERMAL GOLD MINERALIZATION IN THE VELVET DISTRICT,
PERSHING COUNTY, NEVADA

APPROVED:

J. Lirland Kyle

Daniel S Barker

EPITHERMAL GOLD MINERALIZATION IN THE VELVET DISTRICT, PERSHING COUNTY, NEVADA

by

WILMER DALLAM MASTERSON IV, B.S.

THESIS

Presented to the Faculty of the Graduate School of

The University of Texas at Austin

in Partial Fulfillment

of the Requirements

for the Degree of

MASTER OF ARTS

THE UNIVERSITY OF TEXAS AT AUSTIN

December 1981

This thesis is dedicated
to my parents

ACKNOWLEDGMENTS

Bear Creek Mining Company supported field work in June 1980 and provided trace and precious metal analyses. Dr. J. Richard Kyle, my supervisor, and Ray Willcox visited the field area and made many useful suggestions. Dr. Lynton S. Land performed the ^{18}O extractions and analyses, and petrographic assistance was provided by Drs. Daniel S. Barker and Chris Henry. Drs. Kyle, Land, and Barker served on my committee and made helpful editorial suggestions.

Polished doublets for fluid inclusion analyses were prepared by Richard Morales, who also assisted in thin section preparation. Larry Mack instructed me in the use of the SEM. Ralph Kugler served as student editor.

ABSTRACT

Gold mineralization in the Velvet District occurs in an eastward dipping sequence of Miocene tuffs, flows, and tuffaceous sediments on the west flank of the Trinity Range in Pershing County, Nevada. Numerous north-northeast trending normal faults extend through the district. These faults served as conduits for ascending hydrothermal fluids which deposited gold and silver along poorly defined zones of brecciation, argillic alteration, and quartz veining. Concentration of gold does not exceed a few parts per million and is highest in zones of intersecting fractures.

The hydrothermal solutions which deposited the gold were the near-surface expression of a larger geothermal system. Meteoric water leached gold, silver, arsenic, antimony, and other metals from the surrounding rock as it percolated downward towards a deep heat source. The hot fluids escaped upward along fracture zones and precipitated precious metals in veins near the surface. Fluid inclusion studies indicate that the quartz veins were deposited in the temperature range 218-264° C from fluids which had salinities equivalent to 0.2-0.8 weight percent NaCl. $\delta^{18}O$ of quartz veins varies from -2.5 to +6.7 °/oo, and the low values appear to define a zone of concentrated fluid flow and potential subsurface mineralization in the southeast part of the district. The lowest value, -2.5 °/oo, indicates that the ore fluid must have been Tertiary meteoric water with $\delta^{18}O$ equal to -13 °/oo.

Reaction of hydrothermal fluids with wall rock produced an al-

teration assemblage of illite-kaolinite-quartz which underlies most of the shafts, adits, and prospect pits in the district. The illite-kaolinite-quartz assemblage is laterally gradational into a kaolinite (or dickite)-smectite-alunite-quartz assemblage which is indicative of lower temperatures. Pyrite and other sulfides are rare, but limonite and jarosite are widespread in surface outcrops. Alteration of tuffs released abundant silica which precipitated as quartz veins and discharged in hot springs at the bottom of lakes, where thick deposits of diatomaceous earth accumulated.

TABLE OF CONTENTS

LIST OF TABLES

LIST OF FIGURES

LIST OF PLATES

INTRODUCTION

PURPOSE

Many gold and silver deposits were formed by processes that can be observed in modern geothermal areas. Study of fluid chemistry, hydrothermal alteration, trace and previous metal distribution and geologic setting of geothermal areas provides information which can be used to construct an exploration model for the discovery and evaluation of precious metal deposits. Initial geochemical sampling in the Velvet District by Bear Creek Mining Company revealed anomalous, non-economic amounts of precious metals but failed to show any trends to guide further exploration in the area. This thesis was undertaken to study the mineralization in the Velvet District and to develop an exploration model by comparing the district to modern geothermal systems and to other precious metal deposits.

LOCATION

The site of the Velvet gold mines is about 25 km west of Lovelock in Pershing County, Nevada, on the west flank of the Trinity Range (Fig. 1). The halo of hydrothermal alteration associated with gold mineralization is largely confined to Section 6 in Township 27N, Range 29E. No published USGS topographic maps were available for this area in 1980 except for the 1:250,000 scale Lovelock AMS Sheet, but preliminary blue-line 7½' topographic maps were obtained from Federal Offices

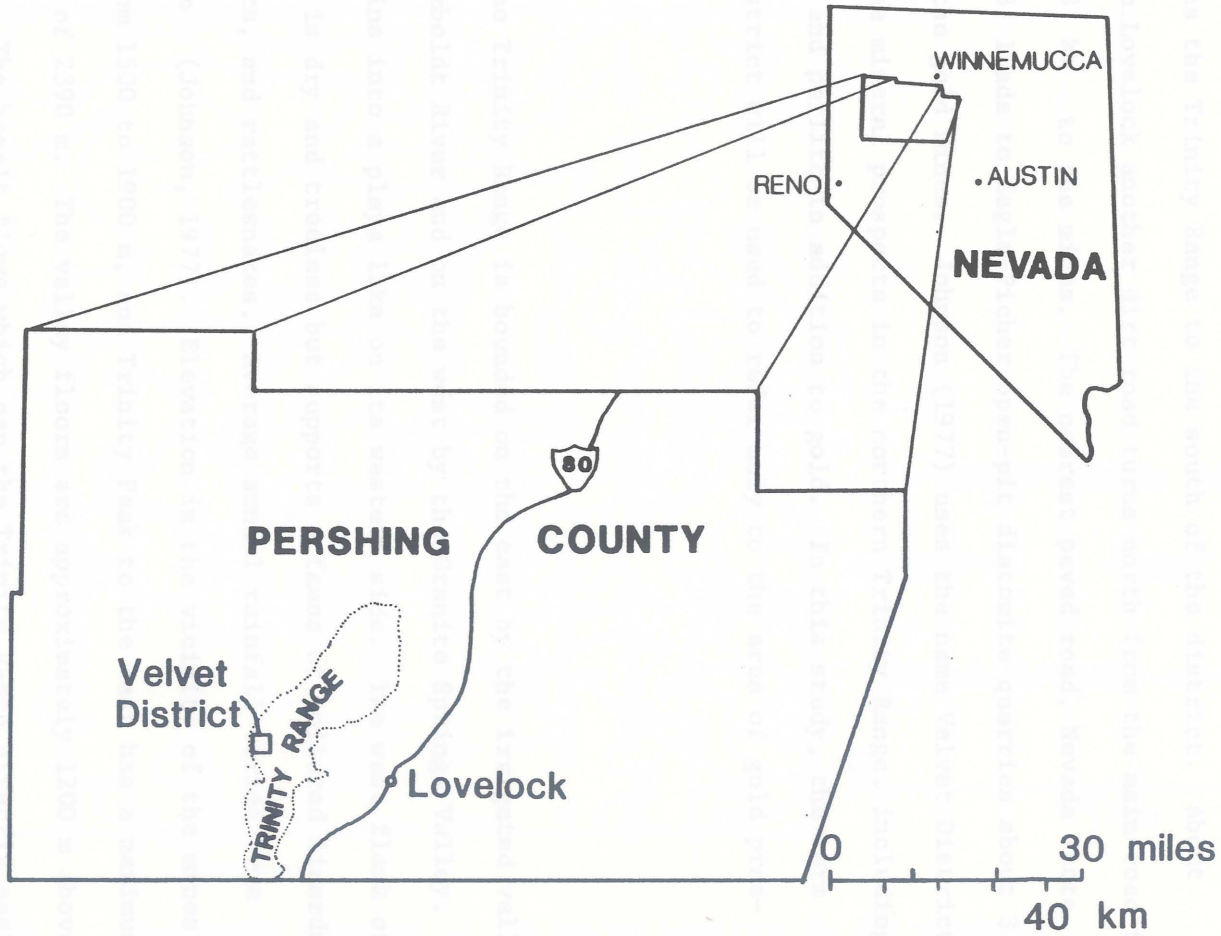

Figure 1. Location map of the Velvet District.

in Reno and used as a base map for this study (Fig. 2). The mines are reached by an unpaved road which proceeds south and west from Lovelock and crosses the Trinity Range to the south of the district. About 32 km from Lovelock another dirt road turns north from the main road for the last 3 km to the mines. The nearest paved road, Nevada State Highway 48, leads to Eagle-Picher open-pit diatomite quarries about 3 km north of the gold mines. Johnson (1977) uses the name Velvet District for all the mineral prospects in the northern Trinity Range, including diatomite and perlite in addition to gold. In this study, the term Velvet District will be used to refer only to the area of gold prospects.

GEOGRAPHY

The Trinity Range is bounded on the east by the irrigated valley of the Humboldt River and on the west by the Granite Springs Valley, which drains into a playa lake on its western side. The west flank of the range is dry and treeless but supports a fauna of collared lizards, jackrabbits, and rattlesnakes. Average annual rainfall varies from 9 to 50 cm (Johnson, 1977). Elevation in the vicinity of the mines ranges from 1500 to 1900 m, and Trinity Peak to the east has a maximum elevation of 2390 m. The valley floors are approximately 1200 m above sea level. The basalt flows which cap the Trinity Range directly east of the mines are covered with lichen that gives them a green appearance when viewed from a distance. At sunset the texture of these flows is said to have resembled velvet to the early prospectors, hence the dis-

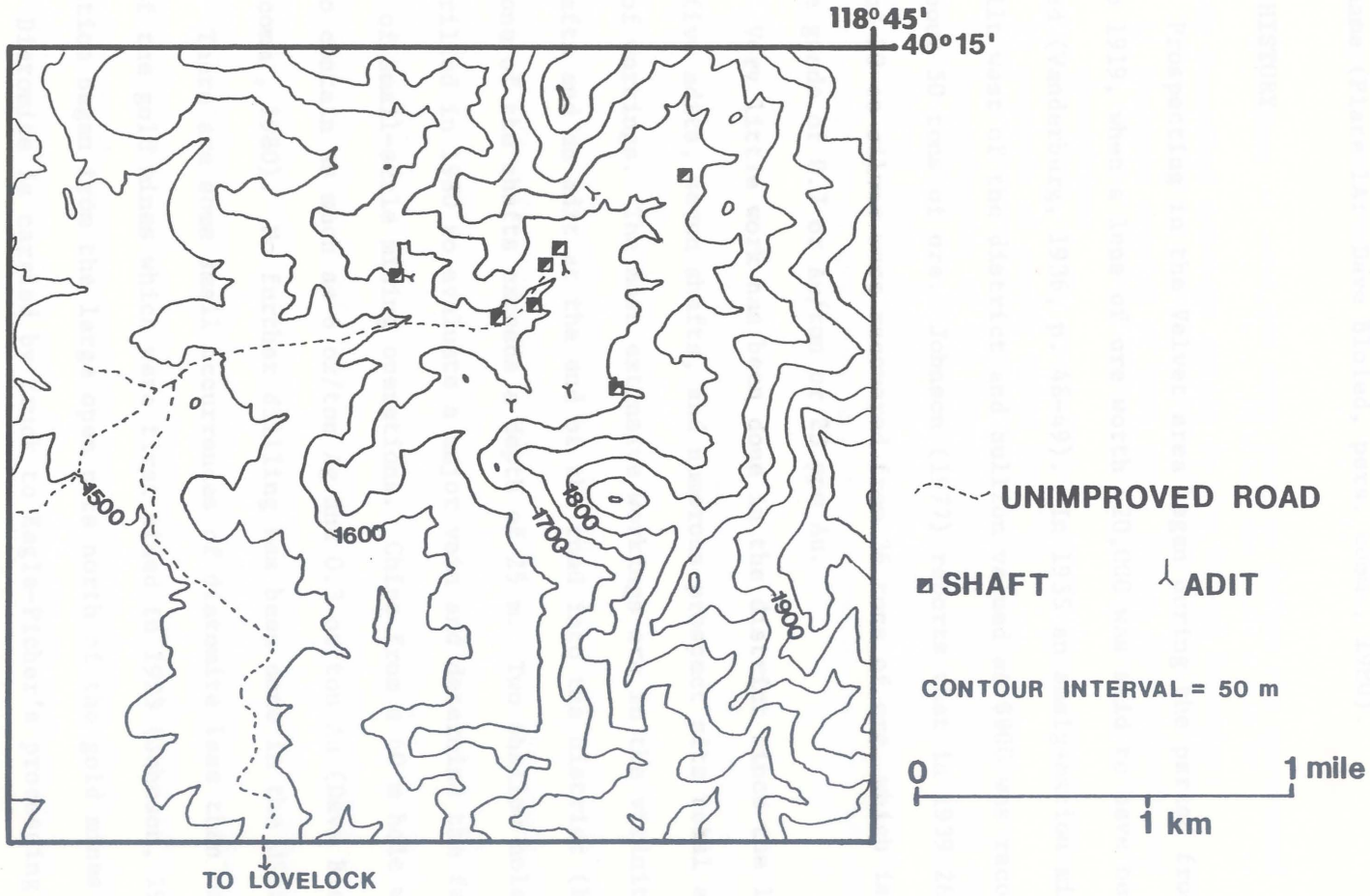

Figure 2. Topographic base map of the Velvet District in the northeast corner of the unpublished USGS 7½' Seven Troughs 3 NE quadrangle.

trict name (Plate 1A; Dave Bloied, pers. comm., 1980).

MINING HISTORY

Prospecting in the Velvet area began during the period from 1915 to 1919, when a lens of ore worth $20,000 was said to have been produced (Vanderburg, 1936, p. 48-49). In 1935 an amalgamation mill was built west of the district and bullion valued at $900 was recovered from about 50 tons of ore. Johnson (1977) reports that in 1939 26 oz gold and 10 oz silver were recovered from 36 tons of ore, which is an average grade of 0.7 oz Au/ton or 23 ppm Au.

Very little work has been done in the district since the 1930s. Today five adits, seven shafts, and numerous prospect pits total about 370 m of workings. The most extensive workings are in the vicinity of two shafts and an adit at the end of the road into the district (Fig. 2). None of the shafts exceeds a depth of 25 m. Two shallow holes were drilled in 1980 to evaluate a major vein and determine the feasibility of small-scale mining operations. Chips from a 60 m hole were said to contain as much as 6 oz/ton Ag and 0.3 oz/ton Au (Dave Bloied, pers. comm., 1980). No further drilling has been done in the district.

There are some small occurrences of diatomite less than one km west of the gold mines which were first mined in 1923 (Johnson, 1977). Production began from the large open pits north of the gold mines in 1952. Diatomite is carried by truck to Eagle-Picher's processing plant on the Southern Pacific Railroad near Lovelock.

METHOD OF INVESTIGATION

Five lines of evidence were used to define the geothermal system which deposited precious metals in the Velvet District:

1) Geologic mapping of host rock, veins, and hydrothermal alteration;
2) Analysis of quartz veins for ^{18}O;
3) Determination of the homogenization temperatures and salinities of fluid inclusions in the quartz veins;
4) Analysis of the trace and precious metal content of altered rock;
5) X-ray diffraction and petrographic study of hydrothermal alteration.

Prior to this investigation, the geology of the district was known only through reconnaissance geologic mapping by the Southern Pacific Company. Detailed geologic mapping of a ten square kilometer area was conducted during June 1980 with financial and logistical support provided by Bear Creek Mining Company. During the course of this mapping, 91 samples of altered rock were selected for gold, silver, lead, and mercury assay, 33 of which were also analyzed for arsenic, antimony, fluorine, and uranium. Eight quartz vein samples were collected for oxygen isotope analysis and fluid inclusion study. Seventy thin sections were cut from both fresh and altered rock to study the effects of hydrothermal alteration upon original textures. Identification of hydrothermal clays was supplemented by X-ray diffraction analysis of 25 samples.

REGIONAL GEOLOGY

The Trinity Range is a typical Basin and Range horst, bounded on the east and west by downdropped alluvium-filled valleys. Tertiary normal faulting tilted the range so that its capping basalt flows now dip eastward. Most of the range is made up of Tertiary volcanic and sedimentary rocks, with scattered exposures of Mesozoic basement. The oldest rocks exposed are the Auld Lang Syne Group, which includes schist, phyllite, hornfels, limestone, and marble of probable Triassic and early Jurassic age (Johnson, 1977). In the extreme southern part of the range in Churchill County there are also exposures of metavolcanic rock of late Paleozoic or early Mesozoic age (Willden and Speed, 1974). These early Mesozoic rocks were metamorphosed during emplacement of Cretaceous granodiorites in the time interval 85 to 104 myBP, within the age range of the younger intrusive phases of the Sierra Nevada and Idaho Batholiths. These granodiorites once formed a continuous chain of batholiths which has been disrupted between California and Idaho by Tertiary volcanism and normal faulting (Hamilton, 1969). Two plutons from the Trinity Range were dated at 90 my (Smith and others, 1971). The Ragged Top and Toy scheelite districts are hosted in tactite along the contact between granodiorite and Auld Lang Syne metasediments in the southern part of the range near the Pershing-Churchill county line.

The bulk of the range is made up of the Miocene and Pliocene tuffs, flows, and tuffaceous sediments which host gold mineralization

in the Velvet District. Unfortunately, these Tertiary units are known only from reconnaissance mapping, and volcanic stratigraphy has not been defined in detail. A Miocene caldera (12 myBP) has been identified at Ragged Top just north of the county line about 20 km south of the Velvet District. This caldera was the source of dacitic to rhyolitic flows which were probably contemporaneous with rhyolite plugs associated with mineralization in the Jessup gold and silver district in Churchill County (Willden and Speed, 1974). Andesites of unknown age (pre-Miocene?) also outcrop in the Jessup District.

North of Ragged Top the Tertiary section is dominated by ash-flow and ash-fall tuffs which interfinger with lacustrine tuffaceous sediments and rhyolite flows and domes. An obsidian nodule from a U.S. Gypsum perlite deposit on the west flank of the range was dated at 23±2 my (early Miocene) by fission track methods (McKee and Marvin, 1973). A rhyolite and quartz latite flow in the same general area yielded ages of about 14 my, which corresponds to the age of mineralization in the Seven Troughs District to the northwest (McKee and Marvin, 1973). It is not known what stratigraphic relationship these dated samples have to the mineralized tuffs and flows of the Velvet mines. Development of basin and range topography began in the interval 17-14 myBP, which also marks the widespread appearance of bimodal basalt-rhyolite volcanism in the Great Basin (Christiansen and McKee, 1978).

GEOLOGY OF THE VELVET DISTRICT

GENERAL STATEMENT

Identification of lithologies and stratigraphy of the gold-bearing volcanic rocks was hampered by hydrothermal alteration in the central part of the district and by faulting throughout the mapped area. Also, because of time limitations it was not possible to extend mapping outside the district in order to relate mineralization to the volcanic and structural history of the range. The abundance of coarse tuffaceous sediments and interbedded flows and tuffs suggests close proximity to a volcanic center, possibly within the moat of a caldera or group of nested calderas.

Gold was precipitated by hydrothermal fluids ascending through eastward-dipping rhyolitic tuffs, flows, and sediments which have been intensely altered and cut by faults of varying orientation (Figs. 3,4). Age of the mineralized rock is uncertain but is probably Miocene, 23-12 myBP. Field evidence suggests that eruption of rhyolite, andesite, and basalt occurred during the initial stages of normal faulting and mineralization in the time interval 14-12 myBP. Extrusion of basalt and normal faulting continued into the Pliocene. Thickness of the exposed volcanic rock in the study area totals about 800 m.

STRATIGRAPHY

TUFF AND TUFFACEOUS SEDIMENT

Ash-flow tuff, water-laid tuff, and tuffaceous sediments are

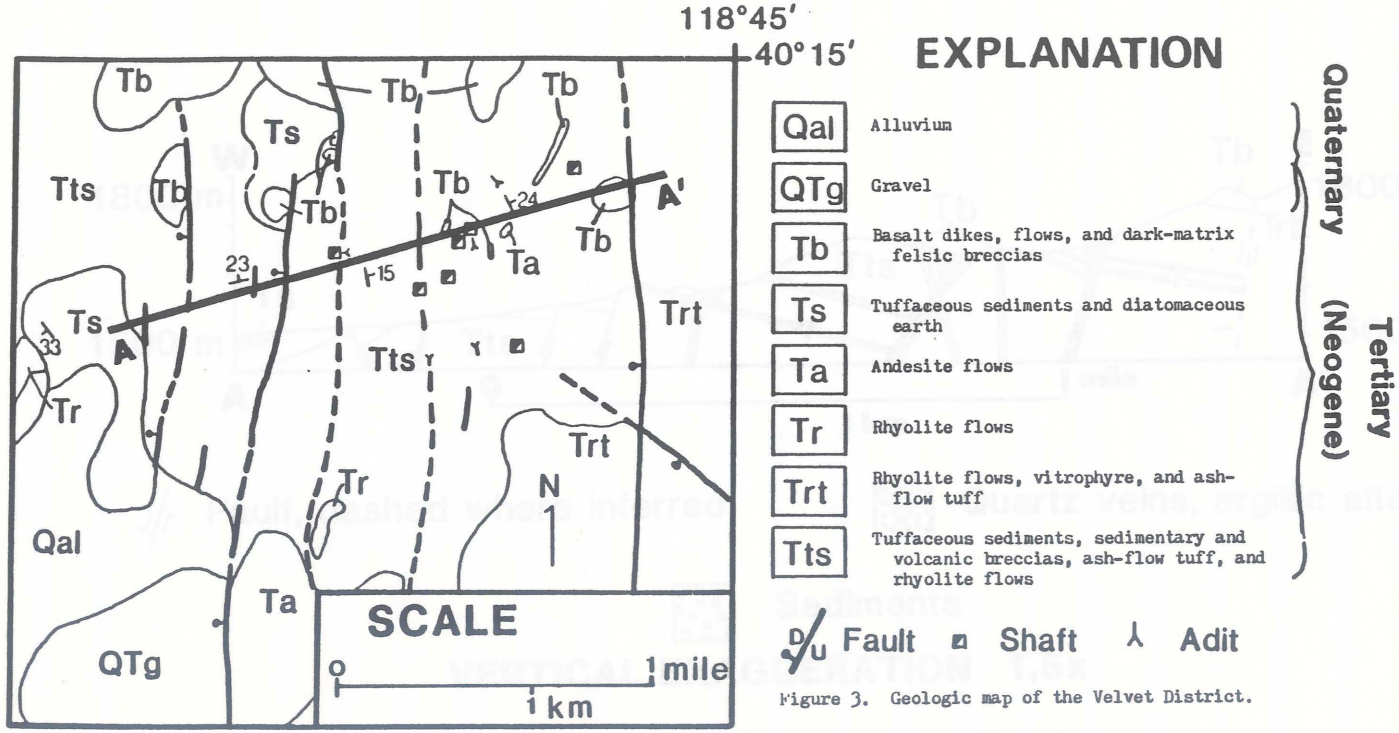

Figure 3. Geologic map of the Velvet District.

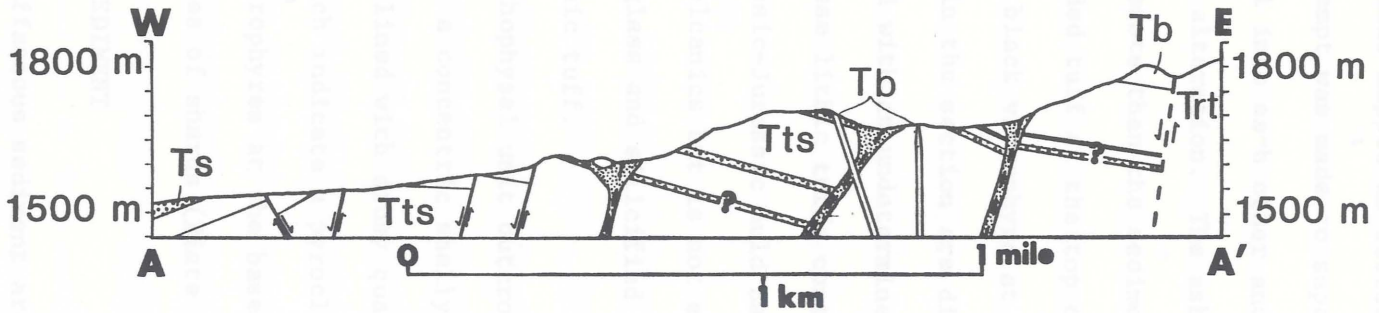

Figure 4. Geologic cross-section A-A'.

all present in the unit mapped as Tertiary tuff and tuffaceous sediment (Tts). No attempt was made to separate the lithologies because they are gradational into each other and are impossible to distinguish in areas of intense alteration. The ash-flow tuffs contain more pumice and exotic fragments than the sediments and are not as well sorted. A red and white banded tuff at the top of the section is about 50 m thick and becomes a black vitrophyre at its base. Thicknesses of lithic tuffs lower in the section are difficult to estimate because they are interbedded with an undetermined amount of sedimentary material. Some of these lithic tuffs contain fragments of phyllite derived from the Triassic-Jurassic Auld Lang Syne Formation which underlies the Tertiary volcanics but is not exposed in the area (Plate 1B). Fragments of green glass and silicified volcanic rock are also common constituents of lithic tuff.

One pink lithophysal unit outcrops in the district (Plate 1C). The lithophysae have a concentric shelly structure with a diameter of about 1 cm, and are lined with drusy quartz. The pink matrix contains compacted shards which indicate a pyroclastic origin. Thin green, brown, and black vitrophyres at the base of thick ash-flow tuffs also contain faint outlines of shards (Plate 3A).

TUFFACEOUS SEDIMENT

Lenses of tuffaceous sediment are interbedded with and grade continuously into the tuffs. Bedding in these sediments is horizontal, but low angle cross-bedding is visible in one thin section. Graded beds are sometimes present (Plate 1D). The sediment in one area con-

tains poorly sorted angular fragments of tuff, pumice, opal, metamorphic rock, perlitic glass, and quartz which are cemented by alunite (Plate 1E). In many areas the sediments are cemented by opal.

Pumice and tuff fragments in the tuffaceous sediments suggest that they are composed of both older eroded fragments and fresh ashfall material that were deposited in lakes during the waxing or waning stages of pyroclastic eruptions. Most of the sediments contain grains no larger than sand size, although one distinctive sedimentary breccia unit is composed of cobble-size clasts of opal and silicified volcanic rock cemented by isopachous opal and chalcedony.

RHYOLITE FLOWS

An unaltered, light purple flow-banded rhyolite outcrops in the southern part of the study area. It contains about 3 percent quartz and sanidine phenocrysts; some of the quartz crystals contain large single and two-phase fluid inclusions (Plate 1F). Abundant tridymite and cristobalite are present in the groundmass. The tridymite is biaxial negative with 2V of about 20 degrees, which conflicts with published data that it is optically positive (for example, Kerr, 1977). Identification of tridymite was verified by X-ray diffraction. Kaolinite coats the tridymite and was apparently deposited as a vapor-phase mineral.

Yellowish spherulitic rocks which outcrop in the altered central part of the district as resistant ridges were tentatively identified as tuffs in the field because of the absence of flow banding (Plate 2A). The yellowish color of the rocks is due to iron-staining

during early stages of devitrification along irregular planes parallel to flow. Iron-bearing vapor-phase mafic minerals (now altered to hematite) fill some of the spherulites within the yellowish devitrified layers. Quartz phenocrysts are usually absent and sanidine is present in amounts up to 10 percent. The sanidine crystals are often zoned and probably contain some sodium, although none of them exhibit the grid twinning characteristics of anorthoclase (Plate 2B).

Other glassy rocks which are probably rhyolite flows outcrop in the western portion of the study area, where they are associated with diatomaceous sediments. One distinctive reddish unit contains about forty percent spherulites in a hematite stained matrix. The hollow spherulites are lined with twinned crystals of tridymite which are coated with hematite and kaolinite in the larger spherulites (Plate 2C). Phenocrysts of feldspar once comprised about ten percent of the rock but were dissolved (during vapor phase activity?) and are now marked by euhedral voids partially filled by kaolinite. The groundmass contains faint outlines which are suggestive of shard structure as well as granophyric quartz-alkali feldspar intergrowths (Plate 2C).

In many cases it was not possible to distinguish between ash-flow tuffs and lava flows with absolute certainty. Exposures of large folds (Plate 2D) are interpreted as slump structures in ash-flow tuff, and flow banding in outcrop or thin section (Plate 2E) identified some rocks as lava flows. In many cases, however, field evidence was either lacking or obscured by hydrothermal alteration, and petrographic examination failed to remove the ambiguities. Some rocks contain squashed

fragments which could be pumice (Plate 2B), yet the presence of flow-aligned trichites in the groundmass and absence of exotic fragments or obvious shards suggests origin as a lava flow. Thick intracaldera ash-flow tuffs can develop textures which mimic those of lavas, including development of granophyric intergrowths in the groundmass. Some of the area mapped as Tertiary tuff and tuffaceous sediment (Tts) includes spherulitic rock of debatable origin which may be lava.

The area shown as Trt on the extreme eastern edge of the map was not studied in detail, but a cursory examination revealed thick sections of spherulitic rock, green glassy flows, and light colored tuffs containing cobble-sized chunks of pumice. The green glass contains spheroidal devitrified bodies which range up to a few centimeters in diameter and are composed of many small coalescing spherulites.

ANDESITE

A fresh andesite flow containing about thirty percent zoned plagioclase phenocrysts outcrops at the extreme southern part of the study area. Estimation of the plagioclase composition by the Michel-Levy method indicates that the resorbed phenocryst cores are bytownite (An_{85}), rimmed by overgrowths of undetermined composition. Some crystals exhibit internal sieve texture. Numerous smaller crystals in the groundmass are oligoclase (An_{10}). The fine-grained matrix is purplish to maroon and contains platy fractures several centimeters long which are filled with tridymite or quartz pseudomorphous after tridymite.

A greenish propylitically altered andesite outcrops in a

small area near the center of the district. It originally contained about thirty percent plagioclase phenocrysts, now altered to calcite. X-ray diffraction analysis indicates that its groundmass has been altered to an assemblage of illite-quartz-K-feldspar and mixed-layer smectite-chlorite.

Andesites have also been reported north of the study area, where they are covered by thick sequences of diatomaceous earth (Johnson, 1977). They are also interlayered with basalts which cover the diatomite, indicating that andesite was erupted during Basin and Range faulting (see section on basalts below), and is mostly younger than the rhyolitic tuffs and flows in the center of the district. The small area of propylitic alteration mentioned above may be part of an intrusive body of andesite.

DIATOMACEOUS EARTH

Diatomaceous earth is the principal lithology in the Tertiary sedimentary rock map unit (Ts). It occurs interlayered with rhyolitic flows in the western part of the map area, where it contains conglomeratic and opalized layers in addition to pure white diatomite. The diatomite is thicker and purer to the north of the district, where deposits several tens of meters thick are mined by open pit. The diatomite is processed by Eagle-Picher Company for use in filters and abrasives.

Examination of a sample of diatomite from Section 1, T27N, R28E with a scanning electron microscope revealed that it is very pure and consists almost entirely of the species Melosira granulata (Plate 3B; Spurr, 1905, p. 69). This species is still alive today and is there-

fore no help in dating the deposits, although they are believed to be of Miocene age (Johnson, 1977, p. 100). The diatoms lived in freshwater lakes which contained abundant silica derived from alteration of the glassy tuffs. Discharge of hot springs at the bottom of the lakes during geothermal activity associated with gold mineralization may have also contributed silica.

BASALT

The youngest volcanic rocks in the study area are olivine basalt flows which have been cut and tilted by north-northeast trending normal faults. Two feeder dikes for these flows also trend north-northeast, suggesting that extrusion of the flows accompanied faulting. Further evidence for the coincidence of volcanism and normal faulting is shown in Plate 3C, in which a tilted, downfaulted basalt is overlain by another almost horizontal basalt flow. The basalts have not been dated but must be younger than the 14 my-old rhyolite and quartz latite flows on the western side of the range because no basalt has been reported to underlie rhyolitic rocks in the Trinity Range.

The basalt flows contain up to ten percent olivine either intergrown with plagioclase in glomeroporphyritic clumps or as isolated skeletal phenocrysts (1-5 mm in length) in the groundmass, similar to other Basin and Range basalts described by Leeman and Rogers (1970). Olivine is partially to totally altered to iddingsite (Plate 3D). Plagioclase phenocrysts are fresh and sometimes exhibit zoning and internal sieving. Of the five flows that were studied petrographically, only one contained clinopyroxene phenocrysts. The groundmass

in all flows contains plagioclase, clinopyroxene, and magnetite or ilmenite, with occasional brown devitrified interstitial glass.

In the northeast corner of the study area dark-matrix felsic breccias and an altered basalt dike outcrop in a northeasterly trending direction. In the dike, olivine and clinopyroxene have been altered to calcite plus chlorite. Plagioclase and magnetite are relatively fresh, however, so the alteration was probably deuteric and not related to mineralization. Unaltered basalt dikes cut veins in some areas, indicating that eruption of basalt began after mineralization ceased.

QUATERNARY SEDIMENT

Quaternary alluvium and gravel fill the valley to the west of the district. Deposition of gravel along fault scarps may have begun during Tertiary time.

STRUCTURE

The tuffs and flows which host gold mineralization dip eastward at about twenty degrees and are cut by north-northeast trending normal faults (Figs. 3,4). The orientations of some large quartz veins (Table 1) are in part parallel to the normal faults, but areas of intense hydrothermal alteration contain at least two sets of veins with differing orientations. This indicates that alteration and mineralization were concentrated in areas of intersecting fractures; normal faults in the western part of the district are commonly silicified but are not cut by cross fractures and are unmineralized. The dip of north-trending veins and basalt dikes varies from 58 degrees to vertical, with

Sample	Vein Orientations
33	N52E,58NW N2E,69E
26	N34E,90 N64E,62N
32	N28E,70N N35W,73SW
15	shear zone trending N42W

Table 1. Orientation of quartz veins measured in the field and taken from a report by A. G. Burritt (1919).

westward dips most common. It is difficult to estimate displacement along faults because alteration obscures lithologic textures and makes correlation across fault planes difficult. Rough calculations suggest that vertical displacement (throw) along a single normal fault is about 200 m, with a total vertical displacement of about 800 m from east to west across Figure 4.

The nearest basalt flow to the north of the altered area is at an elevation 180 m above the level of alteration, suggesting that about 200 m of overburden has been removed from the central part of the district. This is an imprecise estimate because of the widespread faulting, but seems compatible with clay alteration assemblages. An upper limit to the amount of overburden removed is 800 m, which is the difference in elevation between the altered area and the basalt at the peak of the Trinity Range to the east. The basalt flows show evidence of eruption over a topography with some relief, as shown at the base of one flow where cooling joints change from vertical to horizontal where the flow cascaded over a north-south trending fault scarp 50 m high.

GEOLOGIC HISTORY OF THE NORTHERN TRINITY RANGE

Tertiary igneous activity in the Trinity Range began with the Miocene eruptions of voluminous tuff, tuffaceous sediment, and flows upon an uplifted basement of metasediments and Cretaceous granodiorites. Inception of normal faulting in the interval 17-14 myBP was apparently synchronous with development of a mineralizing geothermal system and deposition of diatomaceous earth and rhyolite. Eruption of basalt and andesite continued after geothermal activity ceased. Basalt eruption

eventually ceased in Pliocene or Quaternary time.

HYDROTHERMAL ALTERATION

SILICIFICATION

A zonation of silica types is present in geothermal areas and in epithermal deposits. At the deepest and hottest part of the system quartz is the most abundant form, but chalcedony becomes more prevalent in veins near the surface and opal is precipitated as sinter in surficial hot springs. The solubility of silica is controlled largely by temperature, so the silica supersaturation which leads to opal and chalcedony precipitation is probably caused by cooling of rapidly rising hydrothermal fluids (Buchanan, 1981). In the Velvet District, opal is most common in the western part where it is associated with faults and diatomaceous earth. Chalcedony-quartz veins become more prominent in the eastern part of the map area, where erosion has presumably removed the overlying hot springs deposits.

In the intensely altered eastern part of the district, the rocks are commonly replaced by quartz-clay intergrowths and cut by numerous quartz veinlets. In some areas the original lithology has been completely altered to a homogeneous clay with faintly amethystine quartz crystals lining vugs throughout the clay mass. Large quartz crystals up to 3 cm in length are common in the colluvium in these areas. Isotopic and fluid inclusion analyses of one of these crystals (sample 19) show that it was formed from the same fluids as the quartz veins (Table 2).

Table 2. Hydrothermal alteration products of selected samples. Clays are listed in approximate order of abundance. All altered feldspars are sanidine with the exception of 25 and V25, which also contain plagioclase. Clays exhibiting interference colors no higher than first order gray were identified as smectite; clays with higher-order colors were classified as illite.

Clays were separated from the sample by grinding and gravity settling. X-ray diffraction identification was accomplished with a General Electric XRD-5 diffractometer using nickel-filtered Cu K_{α} radiation at 35 kV and 23 ma.

KEY TO SYMBOLS

Q = quartz
K = kaolinite
I = illite
S = smectite
Mx = mixed-layer clay
D = dickite
A = alunite
lm = limonite or jarosite
C = cristobalite
py = pyrite

Mixed-layer clays are symbolized with a slash if the interlayer minerals are known (e.g. mixed-layer illite/smectite = I/S). In cases where the interlayer composition is not certain, the clays are identified as "Mx".

Sample number	X-ray diffraction identification of clays	Petrographic identification of replacement products: Groundmass	Feldspars
15	Mx	Q,S,py	K,S,Q
17	I,K,S	-	-
20	I/S	Q,lm	S,K,halloysite
25	Mx	S,Q,lm	S
26	I	Q,lm,S	lm,S
27	S,K,I	-	-
31	I	Q,I,py	(none)
33	K,I/S,13Å clay	Q,K,S,lm	S,K,Q
36	K,Mx	-	-
72	Mx	Q,lm	I,lm
78	S	lm	K,S,Q
90	Mx	-	-
92	I,Mx	-	-
94	I	Q,lm	I,Q
6T	K,S	-	-
6T-1	A, α-C	A	(none)
6T-2	K,A, β-C	-	-
8T-8	D,S	-	-
T11	I	I,Q	I
V25	I,Mx	Q,lm	lm,calcite
VM1	I	lm,S	lm

ARGILLIC ALTERATION

Alkali feldspar phenocrysts are typically replaced by quartz, illite, kaolinite, and/or mixed-layer clays in altered areas (Plates 3E, 3F). Clays in groundmass material are usually fine-grained and difficult to identify in thin section. Mixed-layer clays were also difficult to identify by optical methods, so petrographic study was supplemented with X-ray diffraction analysis. The clay fraction was separated by gravity settling in water and then smeared on a glass slide so that the clay flakes would orient themselves parallel to the slide as the water evaporated (Carroll, 1970). A General Electric XRD-5 diffractometer was used to identify the clays with nickel-filtered Cu K_α radiation at 35 kV and 23 ma. All samples were X-rayed once at room temperature and then again after exposure to ethylene glycol vapor at 60° C for one hour. Clays which had basal reflections at about 10 Å and did not expand when glycolated were classified as illite. Clays which had basal reflections in the region of 14-15 Å, expanded to 17 Å upon glycolation, and collapsed to 10 Å after heating, were classified as smectite. Mixed-layer clays gave broad peaks in the region 10.28-15 Å. In most cases it was not possible to identify the interlayered components of the mixed-layer clays without further study, although many of them appear to have 7 Å chlorite components. Kaolinite has a basal spacing of about 7.2 Å which disappears after heating to 550° C for one hour. One sample contains dickite, which has peaks of greater intensity than kaolinite and small additional peaks in the 20-22° 2θ range (Bayliss and others, 1965). An X-ray diffraction pattern of kao-

linite, alunite, and β-cristobalite is shown in Figure 5. Comparison of optical and X-ray identification of clays shows that most mixed-layer clays have optical properties similar to smectite (Table 2, Plate 3F).

The clays in the Velvet District are divisible into two assemblages which appear to have genetic significance: illite-kaolinite-quartz and kaolinite (or dickite)-smectite-alunite-quartz (Fig. 6). Areas of illite-kaolinite-quartz alteration are associated with large zones of quartz veining which were the major conduits of mineralizing fluids along fracture systems. At its edges the illite-kaolinite zone is gradational into mixed-layer clays, kaolinite, and smectite of the second assemblage.

Formation of these two clay assemblages can be explained by analogy to the chemistry of fluids in modern geothermal systems. In felsic reservoirs, deep geothermal fluids are in equilibrium with quartz, potassium feldspar, illite, albite, pyrite, and epidote, and tend to be rich in potassium and sodium (Fig. 7; Ellis, 1970). As these fluids rise and cool, quartz will precipitate and wallrock feldspar will be altered to illite as the stability field of illite expands with decreasing temperature (Rose and Burt, 1979). At temperatures beneath about 250° C mixed-layer illite/smectite will form instead of illite (Eslinger and Saven, 1973), and pure smectite is stable at temperatures beneath about 160° C (Steiner, 1968).

If the fluid boils, CO_2 and H_2S will be given off and the pH and K/H of the remaining liquid will rise. This causes precipitation of calcite and potassium feldspar (adularia) at the level of boiling.

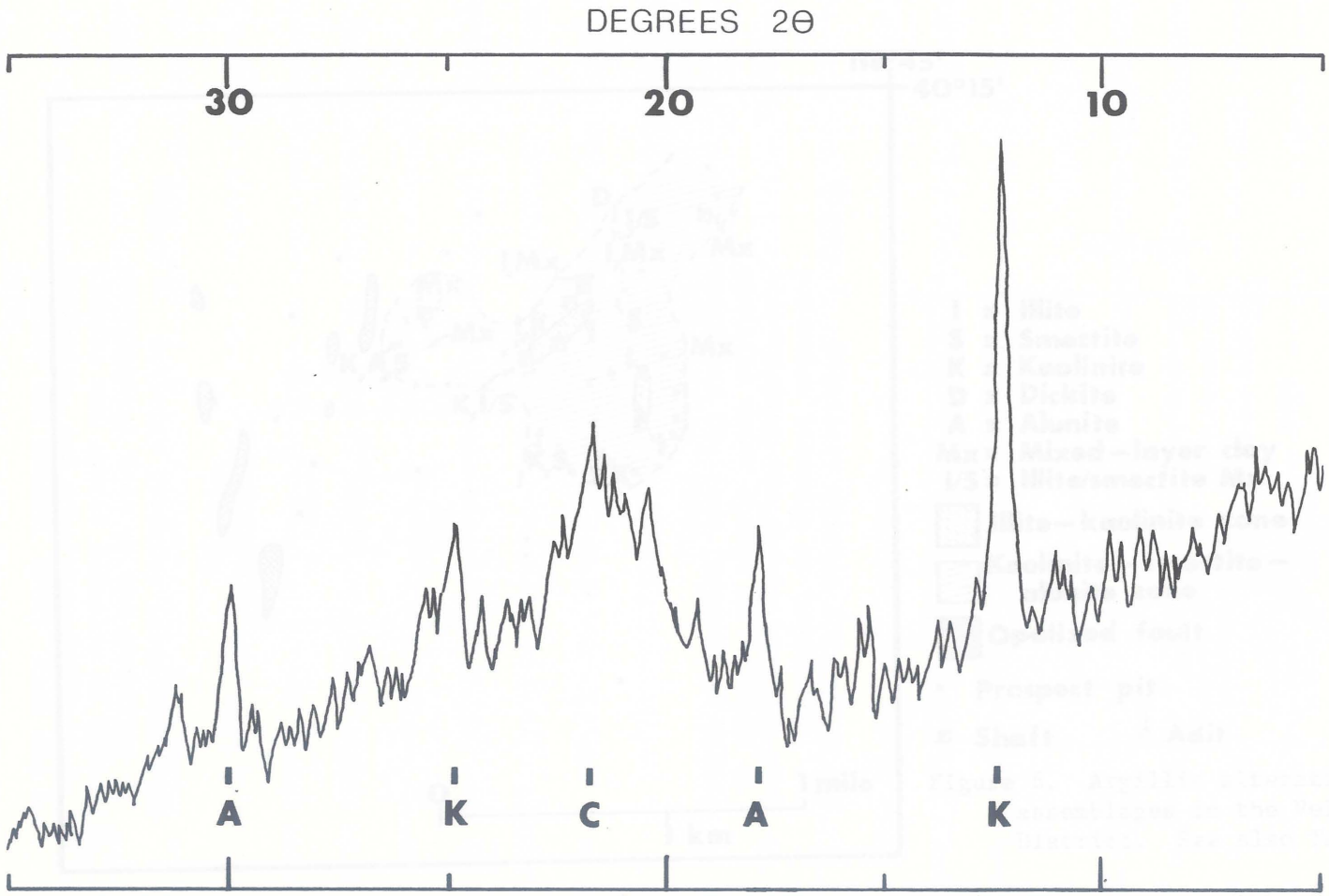

Figure 5. X-ray diffractogram of sample 6T-2 (CuK_{α}).
K = kaolinite, A = alunite, and C = β-cristobalite.

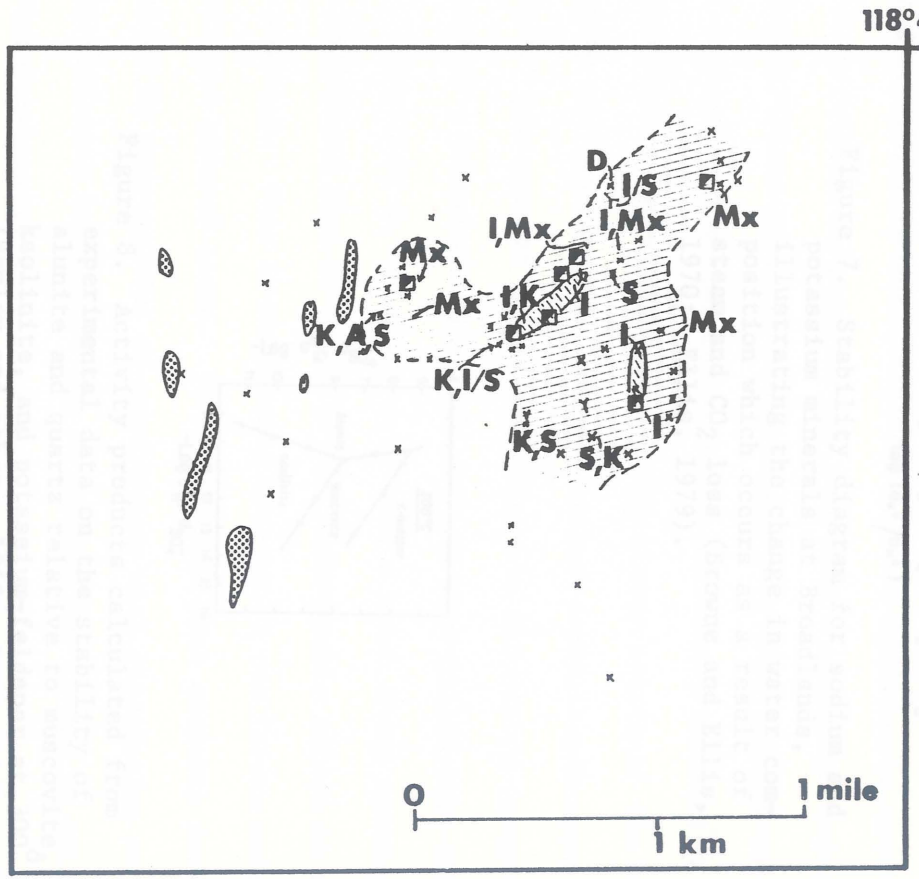

I = Illite
S = Smectite
K = Kaolinite
D = Dickite
A = Alunite
Mx = Mixed-layer clay
I/S = Illite/smectite Mx

Illite-kaolinite zone

Kaolinite-smectite-alunite zone

Opalized fault

× Prospect pit

Shaft Adit

Figure 6. Argillic alteration assemblages in the Velvet District. See also Table 2.

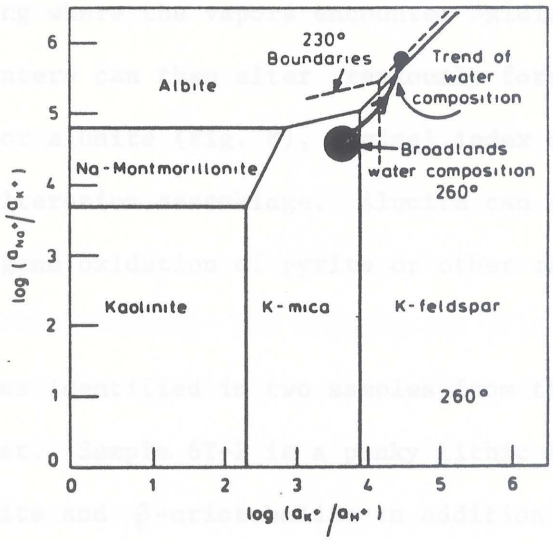

Figure 7. Stability diagram for sodium and potassium minerals at Broadlands, illustrating the change in water composition which occurs as a result of steam and CO_2 loss (Browne and Ellis, 1970; Ellis, 1979).

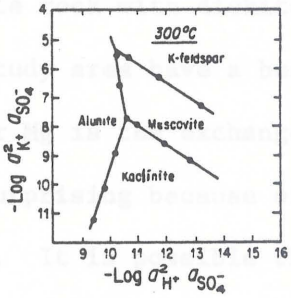

Figure 8. Activity products calculated from experimental data on the stability of alunite and quartz relative to muscovite, kaolinite, and potassium-feldspar at 300° C (Hemley and others, 1969; Rose and Burt, 1979).

Oxidation of H_2S to H_2SO_4 and formation of carbonic acid occur above the zone of boiling where the vapors encounter oxidized surface waters. These acidified waters can then alter previously formed illite to kaolinite, dickite, or alunite (Fig. 8), typical index clays of the advanced argillic alteration assemblage. Alunite can also form by low-temperature supergene oxidation of pyrite or other sulfides (Field and Lombardi, 1972).

Alunite was identified in two samples from the western part of the Velvet District. Sample 6T-2 is a punky lithic tuff which has been altered to kaolinite and β-cristobalite in addition to alunite (Fig. 5). A tuffaceous sediment in the same area contains pore-filling alunite cement (Plate 1E). It seems likely that this alunite was precipitated during low-temperature supergene processes, since high temperature fluids would be expected to attack the glassy matrix of the sediment. Kaolinite and smectite are common in other acid-altered areas in the district. One area of illite/smectite vein alteration (sample 20) is overlain by a bleached white rock with dickite-filled vugs (Plate 4A).

Smectites in the study area have a basal X-ray spacing of about 14 Å, indicating that Ca or Mg is the exchangeable cation in the interlayer position. This is surprising because of the felsic nature of almost all the altered rocks. It is possible that smectite formation took place at near-neutral pH synchronous with dissolution of calcium-bearing silicates but before the pH dropped low enough to attack sodium and potassium-bearing silicates (Schoen and others, 1974). Several samples were altered to greenish clays which appear to be random interstratifications of chlorite and illite or smectite. These clays gave

poor X-ray peaks which were difficult to interpret, and may represent the lowest alteration temperatures in the district. Scarcity of chlorite is probably due to the absence of alterable ferromagnesium minerals.

Pyrite was not abundant in the surface outcrops of the district, but many samples contain iron oxides and hydroxides (limonite) and jarosite. Often the iron-bearing minerals occur as minute spheres scattered throughout the groundmass and phenocrysts (Plate 4B).

The envelope of argillic alteration (Fig. 6) narrows to the south where relatively fresh andesite and rhyolite outcrop. Younger basalts cover the outcrops to the east, and mapping was not extended to the north. The total area of argillic alteration is a little more than 1 km^2, which is comparable to the productive areas of Tonopah, Goldfield, and other epithermal deposits, although these deposits are often associated with much larger areas of barren alteration.

MINERALIZATION

INTRODUCTION

Precious metal deposits which are believed to have formed at near-surface temperatures and pressures are generally classified as epithermal, despite the fact that most were formed at temperatures higher than the 200° C limit set by Lindgren (1933). Fluid inclusions studies indicate that most epithermal ores were deposited from dilute fluids (< 3 weight % NaCl) at typical geothermal temperatures (200-300° C; Nash, 1972). Modern geothermal areas provide an excellent model for epithermal ore deposits, and several geothermal areas contain small amounts of economic metal concentrations (Weissberg and others, 1979).

Most epithermal deposits formed in complexly faulted areas, usually accompanied by igneous activity which provided a heat source to set up fluid circulation in the fractured host rock. As meteoric water percolates downward on the margins of the system it heats up and leaches metals from the surrounding rock before rising along fractures. Gold is believed to be carried in solution as a sulfide or chloride complex and solubilities as high as 546 ppm Au (238° C, 1 kb) have been measured in experiments (Barnes, 1979). Precipitation of precious metals near the surface can be caused by boiling, reaction with wallrock, mixing with cool groundwater, or other mechanisms (Buchanan, 1981; Barnes, 1979). Quartz is the most abundant gangue mineral, precipitating in fissures and breccia zones as the ore solutions rise and cool.

VEINS

A report written by A. G. Burritt in 1919 describes the workings at the two inclined shafts and tunnel at the end of the access road to the Velvet claims. These workings are still open for sampling. Burritt stated that the veins in the workings consisted of iron-stained quartz and altered host rock in six to fourteen-foot (2 to 4.5 m) wide zones with well-defined walls. Quartz was most abundant near the walls but was also present throughout the width of the veins. Gold was said to be associated with the quartz and in the altered wallrock surrounding the veins.

Material in the dumps and prospect pits in the district is usually argillized and may contain small quartz veinlets up to a few millimeters in thickness. In some samples the quartz veinlets cross-cut and are therefore younger than zones of argillic alteration (Plate 4C), but in most cases veinlets are surrounded by an envelope of argillation which appears to have formed synchronously with the quartz. The veinlets sometimes form an anastomosing network and usually do not have any measureable orientation. Banded quartz veins such as shown in Plate 4D are uncommon. This vein contains at least three generations of euhedral comb quartz separated by brecciated, sugary microcrystalline quartz. Intergrowths of wedge-shaped adularia are partially replaced by jarosite along cleavage planes (Plate 4E).

Vein quartz usually has a sugary appearance caused by continuous brecciation and movement during crystallization from hydrothermal solutions. Breccia fragments are often replaced by microcrystalline or

flamboyant quartz, and some veins contain feathered quartz (Plate 4F). The space between fragments is sometimes lined with quartz prisms growing out perpendicular to a fragment in a comb structure. Larger quartz crystals in brecciated rock commonly show evidence of strain, such as undulose extinction, grid-like twinning pattern, or inclusion-filled fracture planes. Even clear euhedral crystals growing into open space are usually cut by fracture planes which have necked down to form planes of secondary fluid inclusions.

The quartz morphologies described above are typical of surficial veins (Adams, 1920). The veins in the district are unusual in that they contain very little material other than quartz and clay. This may mean that erosion has exposed only the silicified upper portion of the vein system. Less optimistically, lack of other minerals may mean that the geothermal fluids were metal-poor, although salinity of fluid inclusions in the district is comparable to salinities in ore deposits elsewhere. Small euhedral pyrite crystals are intergrown with quartz and are also scattered throughout argillized portions of veins. Pyrite is partially or completely oxidized to iron oxides and hydroxides in surface exposures, often imparting a yellowish color to the rock. Carbonate minerals were not seen in any dumps. Adularia is also rare and no large crystals were seen in the veins.

FLUID INCLUSIONS IN QUARTZ

Eight quartz samples were selected for study of their fluid inclusions on a Chaixmeca microthermometry apparatus. Clear, euhedral

quartz crystals were used whenever possible because milky vein quartz was found to contain a myriad of healed fractures with very few primary inclusions. Samples were cut to a thickness of 1 mm or less, polished on both sides, and studied petrographically to identify areas of inclusions which were then cut into small fragments to fit on the heating and freezing stage. The stage was calibrated with standards of known melting point, as outlined by Roedder (1976). Size of bubbles was measured before and after heating or freezing, and the samples were rerun to ensure that no leakage occurred during the initial run.

Salinity determinations were made by freezing the inclusion fluids with liquid nitrogen vapor and allowing the sample to warm at room temperature until the ice disappeared. The observed freezing-point depressions ranged from -0.4 to -0.1° C, which corresponds to salinities of 0.8 to 0.2 weight percent NaCl (Table 3). The true fluid salinities are probably in the least saline range of these values because the freezing point depressions of -0.1 to -0.8° C observed in quartz crystals from the Broadlands geothermal area suggest salinities that are higher than the actual value of 3000 ppm dissolved solids. The discrepancy vanishes, however, if dissolved CO_2 in the subsurface fluids is taken into account.

After freezing measurements were completed, the samples were heated until the vapor bubble disappeared. This homogenization temperature must be corrected for pressure, however, to yield the true temperature of quartz formation. Since the pressure correction is only about +6° C per km of hydrostatic head (Nash, 1972), it would increase the

Sample	Description	$\delta^{18}O_{SMOW}$ (°/oo)		Homogenization temperatures (°C) Primary inclusions	Secondary inclusions	Salinity (wt. % NaCl)
19	faintly amethystine, euhedral xl (1 cm) projecting into vug	+3.89 +4.19	+4.0	218,244	-	0.8
26	4 cm vein with 3 generations of quartz; sample from youngest quartz (1 cm)		-2.5	-	136-271	0.4
33	euhedral xls (4 mm) from thin (1 cm) quartz veins		+4.6	239	-	0.4
69	euhedral xls (3 mm) from center of 1 cm thick vein		+5.8	-	195-272	0.2-0.4
72	euhedral xl (6 mm) projecting out from silicified substrate	+6.63 +6.79	+6.7	245,242	200-233	0.4
78	euhedral xls (1 cm) in thin (3 mm) veinlet		+3.6	237,250	150-252	0.2-0.8
90	thin (3 mm) veinlet; no euhedral xls	+4.77 +4.84	+4.8	-	-	-
94	euhedral xls (7 mm) from 2 cm wide pods of silicification		+2.2	259,264	301,317	0.4

Table 3. $\delta^{18}O$, homogenization temperatures, and salinities of eight quartz samples from the Velvet District. Dr. Lynton S. Land performed the ^{18}O analyses. Homogenization temperatures are not corrected for pressure.

temperatures of Table 3 by only a degree or two if only 200 m of overburden has been removed from the district.

All the quartz samples contained an abundance of inclusions, but most of them were in planes along healed fractures in the crystals. The fluids in these secondary inclusions were probably very similar in temperature and salinity to the fluids in primary inclusions which formed during crystal growth, but during the processes of fracture healing and cooling the secondary inclusions tend to neck down and form smaller inclusions with variable fluid/gas ratios (Roedder, 1979). Because of this effect, the homogenization temperatures of secondary inclusions will show a greater range than primary inclusions.

Isolated large inclusions, far removed from secondary fracture planes, were considered to be primary. These inclusions often had negative crystal shapes and were elongate parallel to crystal growth faces (Plate 5A). Many inclusions were empty or only slightly wet by fluids, which suggests that the fluids were boiling during quartz deposition (Plate 5C; Roedder, 1970). This is to be expected because the shallow temperature gradients in many geothermal areas are close to the boiling curve for pure water (Fig. 9; White and others, 1971).

Nine primary inclusions in the Velvet District have homogenization temperatures varying from 218 to 264° C, with an average value of 244° C, similar to most epithermal precious metal deposits (Nash, 1972). Nineteen secondary inclusions show a much greater spread in homogenization temperatures, from 136 to 317° C. The geographic distribution of primary inclusion temperatures indicates that the fluids were at about

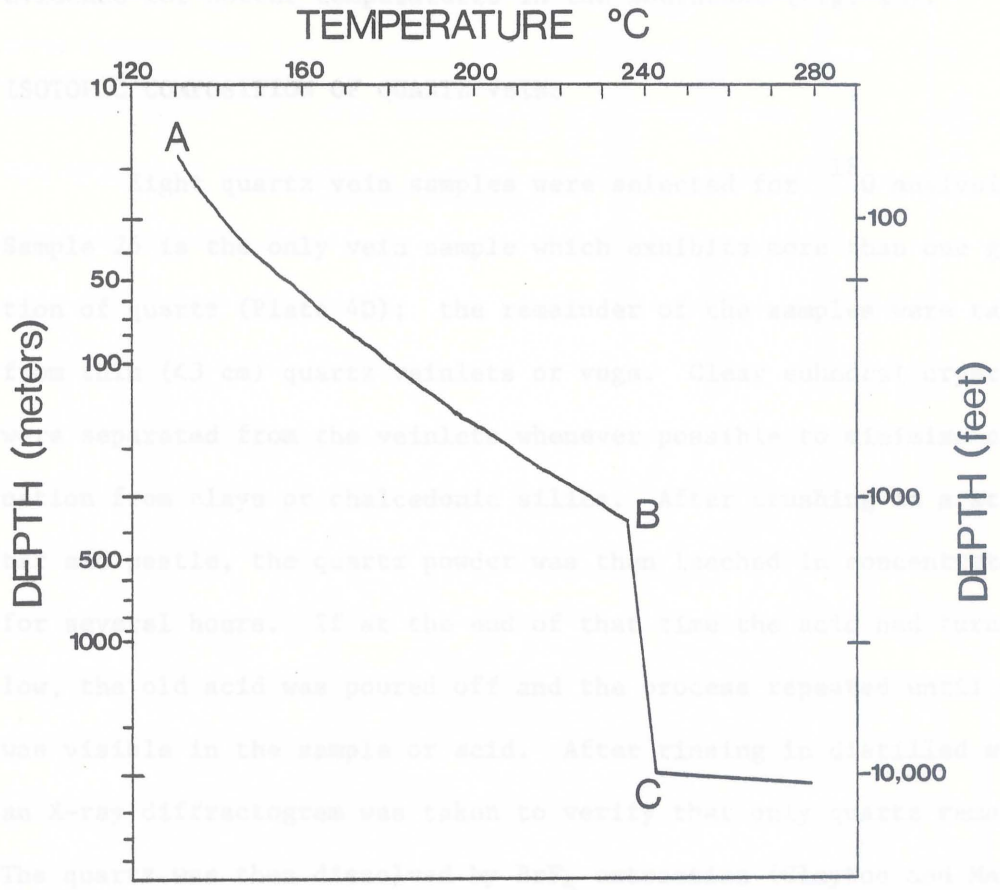

Figure 9. Temperature variation with depth at the Geysers geothermal field in California. Segment A-B is the hydrostatic boiling-point curve for pure water; segment B-C is the temperature distribution in the 2 phase vapor-dominated reservoir; curve below C is the approximate temperature below a hypothetical brine water table at 3000 m depth (White and others, 1971).

the same temperature everywhere in the district, although there is some evidence for hotter temperatures in the southeast (Fig. 10).

ISOTOPIC COMPOSITION OF QUARTZ VEINS

Eight quartz vein samples were selected for ^{18}O analysis. Sample 26 is the only vein sample which exhibits more than one generation of quartz (Plate 4D); the remainder of the samples were taken from thin (<3 cm) quartz veinlets or vugs. Clear euhedral crystals were separated from the veinlets whenever possible to minimize contamination from clays or chalcedonic silica. After crushing in a steel mortar and pestle, the quartz powder was then leached in concentrated HCl for several hours. If at the end of that time the acid had turned yellow, the old acid was poured off and the process repeated until no color was visible in the sample or acid. After rinsing in distilled water, an X-ray diffractogram was taken to verify that only quartz remained. The quartz was then dissolved by BrF_5 extraction (Clayton and Mayeda, 1963) and analyzed for ^{18}O. Results are reported relative to the SMOW standard (Table 3).

Isotopic analyses of D and ^{18}O in quartz veins, adularia, and altered volcanic rock in many epithermal deposits have shown that the ore fluids must have been predominantly meteoric water, although one district (the Comstock Lode) does show evidence of magmatic water in its deeper levels (O'Neil and Silberman, 1974). Magmatic water escaping from a body of cooling igneous rock should have $\delta^{18}O$ values in the range +6–+10 $^{o}/oo$ (Taylor, 1968). Most epithermal quartz veins, how-

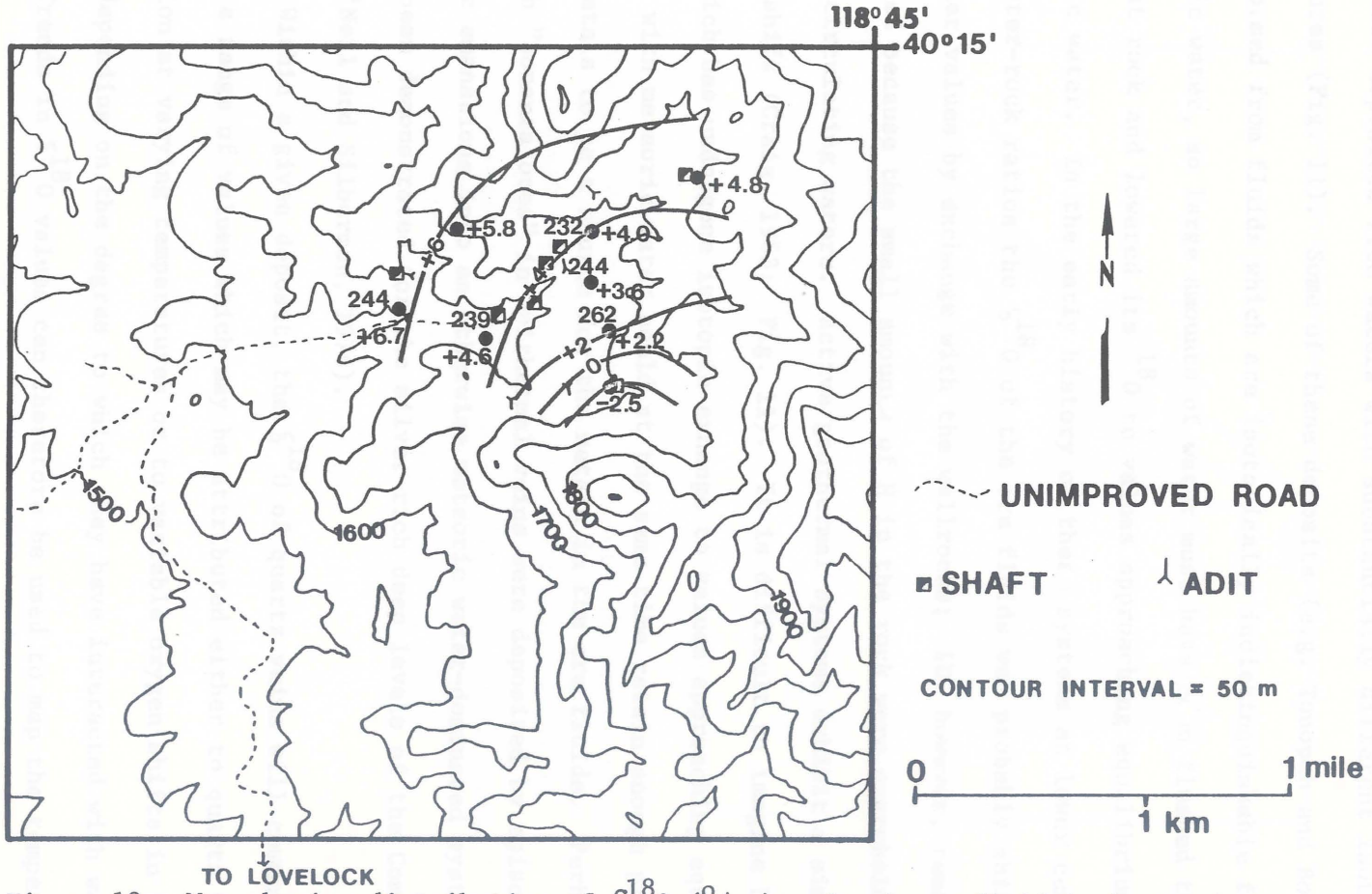

Figure 10. Map showing distribution of $\delta^{18}O$ (°/oo) and primary fluid inclusion homogenization temperatures (°C) of 8 quartz veins in the Velvet District. The $\delta^{18}O$ contours define an area of high water/rock ratios in the southeast.

ever, were deposited from waters with substantially different isotopic signatures (Fig. 11). Some of these deposits (e.g. Tonopah and Bodie) were formed from fluids which are isotopically indistinguishable from meteoric water, so large amounts of water must have been flushed through the host rock and lowered its ^{18}O to values approaching equilibrium with meteoric water. In the early history of these systems at lower cumulative water-rock ratios the $\delta^{18}O$ of the ore fluids was probably shifted to higher values by exchange with the wallrocks; δD, however, remained unchanged because the small amounts of H in the rock were overwhelmed by the circulating waters. Active geothermal systems exhibit a similar oxygen shift (Craig, 1963; Fig. 11). It is difficult to imagine how rock which has undergone isotopic exhange to values approaching equilibrium with meteoric water could at the same time retain enough precious metals to be a source for the metals in the ore fluids. Perhaps the rich "bonanza ores" in epithermal veins were deposited by episodic magmatic emanations into an otherwise meteoric water-dominated system, as has been demonstrated for the silver-rich deep levels of the Comstock Lode (O'Neil and Silberman, 1974).

Within a given deposit, the $\delta^{18}O$ of quartz veins will commonly exhibit a range of values which may be attributed either to quartz precipitation at varying temperatures or to variable oxygen shifts in the fluids depending on the degree to which they have interacted with wallrock. Trends in $\delta^{18}O$ values can therefore be used to map the temperature distribution and/or zones of greatest fluid flow in the system (Fig. 12). At the Tonopah gold and silver deposit, a plot of $\delta^{18}O$ in altered volcanic host rock makes a circular pattern with lowest $\delta^{18}O$

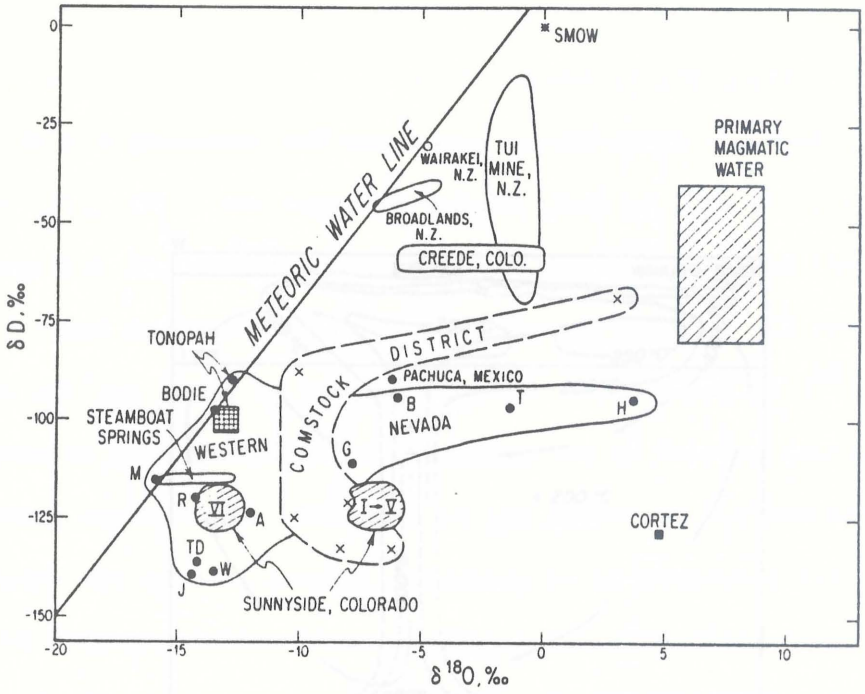

Figure 11. Plot of δD in fluid inclusions versus calculated $\delta^{18}O$ values of hydrothermal fluids in epithermal deposits and active geothermal systems. Note the oxygen shift of geothermal waters at Steamboat Springs and Broadlands and the presence of magmatic water in one sample from the deep levels of the Comstock Lode (Taylor, 1979).

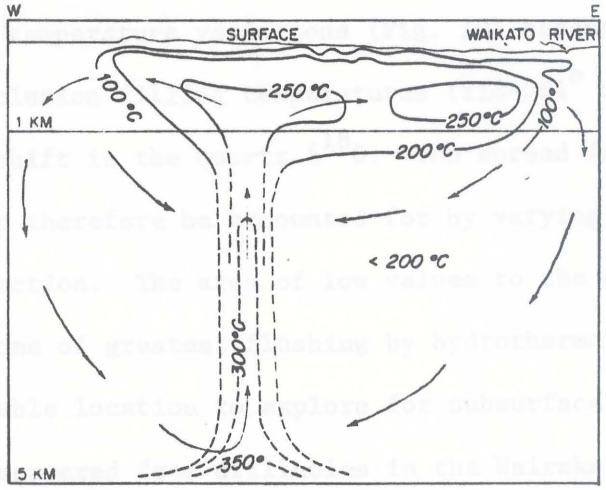

Figure 12. Vertical temperature distribution at the Wairakei geothermal system, New Zealand. Solid isotherms contour measured temperatures; dashed isotherms are estimated (Taylor, 1974).

values over the apex of the productive ore zone (Figs. 13A, 13B; Taylor, 1974).

In the Velvet District, $\delta^{18}O$ content of the quartz veins is lowest in the southeast and increases to the north and west in a regular fashion (Fig. 10). The range in values, from -2.5 to +6.7, cannot be accounted for by temperature variations (Fig. 10) because the range in primary fluid inclusion filling temperatures (218-264° C) would cause at most a 3 °/oo shift in the quartz $\delta^{18}O$. The spread in $\delta^{18}O$ exhibited in Figure 10 must therefore be accounted for by varying degrees of water/rock interaction. The area of low values to the southeast probably marks the zone of greatest flushing by hydrothermal fluids, which would be a favorable location to explore for subsurface ore.

Quartz recovered from drillholes in the Wairakei and Broadlands geothermal areas, New Zealand (Table 4), is nearly in equilibrium with local meteoric water, since the quartz-water fractionation varies from +12 to +7 °/oo in the temperature range 200-300° C (all quartz-water fractionation factors in this report are calculated from the relationship $1000 \ln \alpha = 3.38 \times 10^6 T^{-2} - 2.9$; Friedman and O'Neil, 1977). Quartz veins at Tonopah, Bodie, and Goldfield were also precipitated from isotopically unaltered meteoric water. At Tonopah and Bodie this was confirmed by analysis of D in fluid inclusions which implied a $\delta^{18}O$ of -13 °/oo, with the assumption that the Tertiary meteoric water line was identical to the modern relationship of $\delta D = 8\delta^{18}O + 10$ (Craig, 1961). Taylor (1968) concluded that $\delta^{18}O$ of meteoric waters was in the range -13 to -14 °/oo over much of western Nevada, but O'Neil and Silberman (1974) found evidence for more local variation of $\delta^{18}O$ similar to the

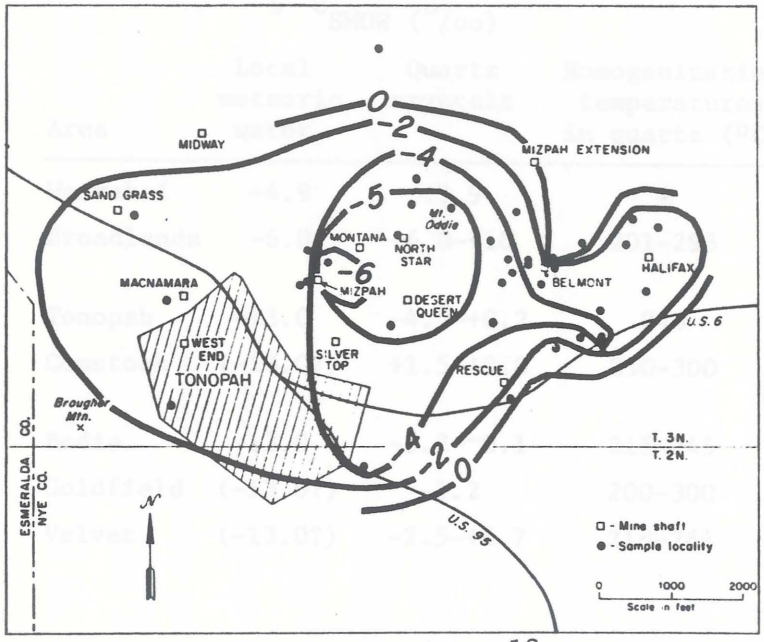

Figure 13A. Map of whole-rock $\delta^{18}O$ of altered volcanic rocks in the Tonopah mining district, Nevada. The contours are roughly similar to the ore horizon contours shown in Figure 13B (Taylor, 1973, 1974).

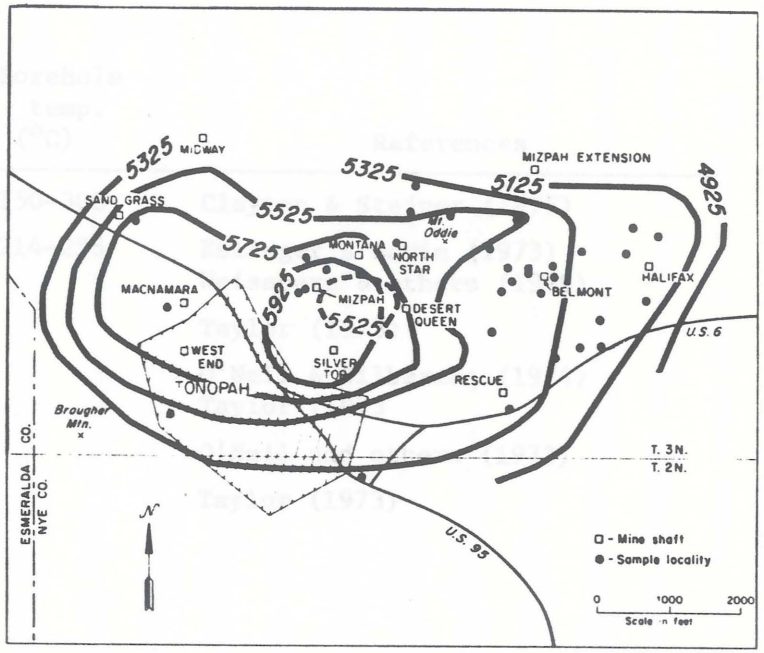

Figure 13B. Map showing the elevation (in feet) above the productive ore zone at Tonopah. The single broken contour at 5525 feet represents the elevation of the apex of the bottom surface of this ore zone (Taylor, 1973, 1974).

Area	$\delta^{18}O_{SMOW}$ (°/oo) Local meteoric water	Quartz crystals	Homogenization temperatures in quartz (°C)	Borehole temp. (°C)	References
Wairakei	-4.9	+3.9	-	150-300	Clayton & Steiner (1975)
Broadlands	-6.0	+6.0-+10	201-293	214-256	Eslinger & Savin (1973) Weissberg & others (1979)
Tonopah	-13.0	-4.5-+0.2	240		Taylor (1973)
Comstock	(-13.0?)	+1.5-+9.0	250-300		O'Neil & Silberman (1974) Taylor (1973
Bodie	-13.0	-3.2-⁻0.1	215-245		O'Neil and others (1973)
Goldfield	(-13.0?)	-1.2	200-300		Taylor (1973)
Velvet	(-13.0?)	-2.5-+6.7	218-264		

Table 4. $\delta^{18}O$ and fluid inclusion data illustrating the similarity of the Velvet District to other epithermal deposits and active geothermal systems. Most of the fluid inclusion homogenization temperatures from epithermal deposits are taken from Buchanan (1981) and have not been corrected for pressure.

present day pattern in the Great Basin. If block faulting did not begin in the Great Basin before Pliocene time, there is no reason to expect that the early Tertiary $\delta^{18}O$ pattern should be similar to the modern distribution, and a value of -13 °/oo was assumed for the Tertiary meteoric waters in the Velvet District. At 244° C, the average homogenization temperature of primary fluid inclusions in the Velvet District, quartz in equilibrium with -13 °/oo water should have $\delta^{18}O$ equal to -3 °/oo, in close agreement with the value of -2.5 °/oo in the late-stage quartz of sample 26. Most of the quartz in the district is heavier than this, so the hydrothermal fluids must have been enriched in ^{18}O by exchange with wallrock. This is understandable in light of the narrow nature of most of the sampled veins, which would not have allowed the ascending fluids to be protected from reaction with wallrock.

GEOCHEMICAL SIGNATURES OF THE MINERALIZING FLUIDS

Ninety-six samples were collected in the field and analyzed for gold and silver to determine the tenor of mineralization. Certain "pathfinder" elements which are often associated with precious metal mineralization were also selected for analysis because they occur in higher concentrations than gold and may be distributed in a halo around gold mineralization. The commonly observed association of gold with Sb, As, Te, Se, and Bi in epithermal deposits may be due to complexing of gold with aqueous species containing these elements, although chloride and sulfide complexes are believed to be the dominant transporters of gold in hydrothermal solutions (Barnes, 1979, p. 430). Goldschmidt

(1954) suggests that gold might be associated with these elements because their large ionic radii (~2Å) permit capture of gold atoms in their crystal structures. Several modern geothermal systems have been observed to form near-surface precipitates rich in Au, Ag, Sb, Hg, and Te (Weissberg et al., 1979). Amorphous antimony sulfide ("metastibnite") containing up to 85 ppm gold has precipitated at Steamboat Springs, Nevada, and Broadlands, New Zealand (White, 1967; Weissberg, 1969).

Lead and mercury values were determined for all 96 samples, and 33 samples containing at least 0.1 ppm gold were also analyzed for arsenic, antimony, uranium, and fluorine. Sampling was biased towards silicified and argillized rock; 56 of the original 96 samples showed obvious quartz veining or argillic alteration.

Hunter Mining Laboratory (Sparks, Nevada) performed the analyses for gold, silver, lead, arsenic, and antimony using atomic absorption spectrophotometry; mercury was analyzed by flameless atomic absorption. Skyline Labs (Denver, Colorado) analyzed for fluorine by specific ion electrode and for uranium by fluorescence techniques.

Trace and precious metal contents of the gold deposits at Carlin and Goldfield are presented in Table 5 as a standard of comparison for the Velvet District.

GOLD

Figure 14 shows the geographic distribution of samples containing more than 0.1 ppm gold, the threshold of detection. Actual concentrations at each sample point are not shown because they are the pro-

	Carlin		Goldfield			
	M	UM	Silicified	Argillized	Ore	Velvet
Au	9	.04	1.3	.11	7.3	*
Ag	0.3	-	0.5	-	30	*
Hg	31	20	0.14	.09	3.9	3.9
As	600	200	30	1.0	3200	312
Sb	150	100	n.d.	n.d.	1500	11
Pb	30	7	10	10	300	32

* = Proprietary data. All values are ppm.

M = Mineralized; UM = Unmineralized; n.d. = not determined

Table 5. Comparison of trace and precious metal concentrations in the Carlin, Goldfield, and Velvet Districts. Values are not strictly comparable because of differences in analytical techniques, methods of sample selection, and methods of averaging, but serve to give a general idea of the magnitude of the anomalies. Velvet analyses are given only for samples containing greater than 0.1 ppm Au. Carlin data are from Akright and others (1967); Goldfield data are from Ashley and Albers (1975).

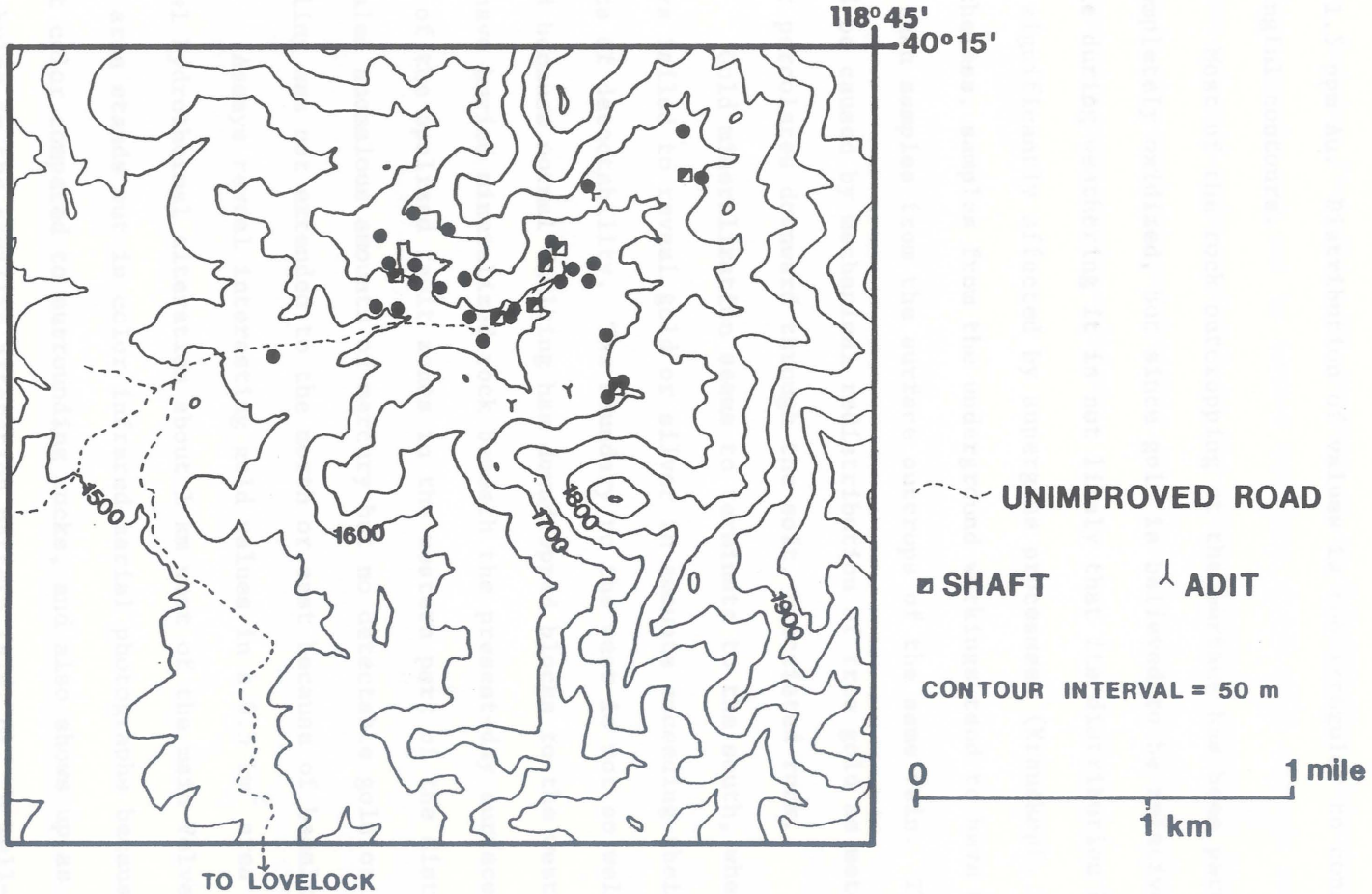

Figure 14. Map showing distribution of samples containing at least 0.1 ppm gold.

prietary data of Bear Creek Mining Company. No sample contained more than 1.5 ppm Au. Distribution of values is too irregular to construct meaningful contours.

Most of the rock outcropping at the surface has been partially to completely oxidized, but since gold is believed to be relatively immobile during weathering it is not likely that its distribution has been significantly affected by supergene processes (Krauskopf, 1967). Nonetheless, samples from the underground workings tend to have more gold than samples from the surface outcrops of the same vein. This could be caused by mechanical redistribution of free gold as meteoric water percolates downward through the soft, brecciated rock.

Gold mineralization seems to terminate to the south, where ten assays failed to reveal gold or silver in amounts exceeding their lower limits of detectability. The boundary to the west is not so well defined because normal faulting has downdropped blocks to the west and may have buried mineralized rock beneath the present-day surface. Assays of the opalized fault zones in the western part of the district revealed anomalous amounts of mercury but no detectable gold or silver. Sampling was not extended to the north or east because of basalt cover.

Assays reveal interesting gold values in a 0.5 km^2 area of surficial hydrothermal alteration about 1 km west of the main Velvet claims. This area stands out in color infrared aerial photographs because of its light color compared to surrounding rocks, and also shows up as a westward bulge in the argillic alteration pattern (Fig. 6). A well-defined northwest trending shear zone in the center of the altered area has been

explored by one adit and several prospect pits along its surface outcrop. Samples from the adit contain up to 0.8 ppm Au. Outcrops of rhyolite nearby are cut by quartz veinlets which also contain small amounts of gold. In contrast to the more competent rhyolite flows, the tuffs in the area are pervasively argillized and silicified but do not contain discrete quartz veinlets.

SILVER

The average Ag/Au ratio (calculated only for samples containing at least 0.1 ppm Au and 1 ppm Ag) in the analyzed samples is 13. Silver values are all below 10 ppm and do not form any regular geographic distribution. Gold-silver ratios do not show any systematic variation with elevation. This may be due to supergene redistribution of the silver, which is more mobile than gold during weathering (Ashley and Albers, 1975, p. A32).

ANTIMONY

The antimony-gold correlation is the highest among the seven pathfinder elements selected for analysis in the Velvet District. Average antimony concentration in rock containing at least 0.1 ppm gold is 11 ppm (Fig. 15; Table 5).

ARSENIC

Arsenic concentrations average 312 ppm and show a greater range than those of antimony (Fig. 16). With one exception, all samples containing greater than 100 ppm As also contain more than 0.1 ppm Au.

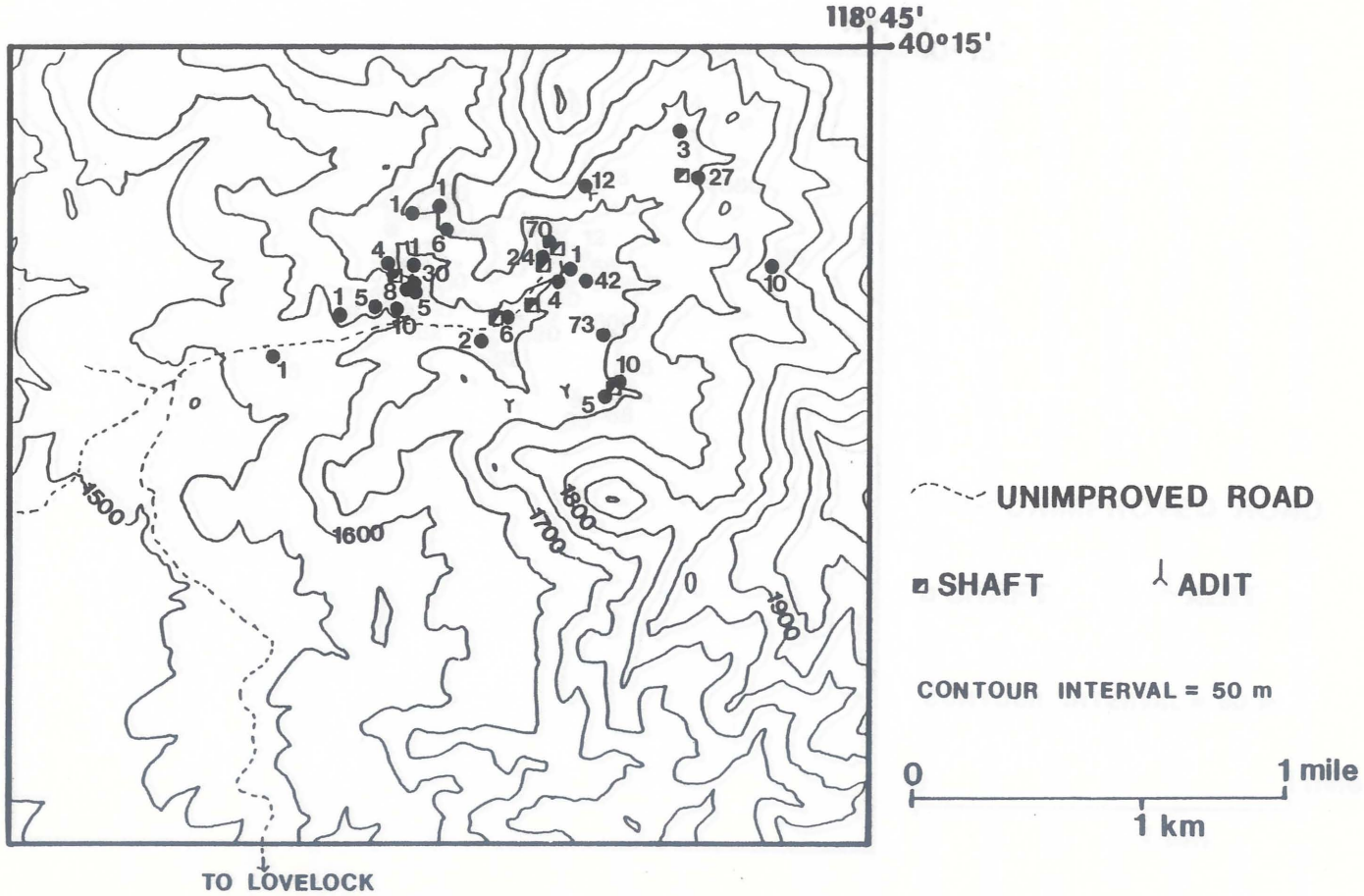

Figure 15. Map showing distribution of antimony in samples containing at least 0.1 ppm gold. Values are ppm.

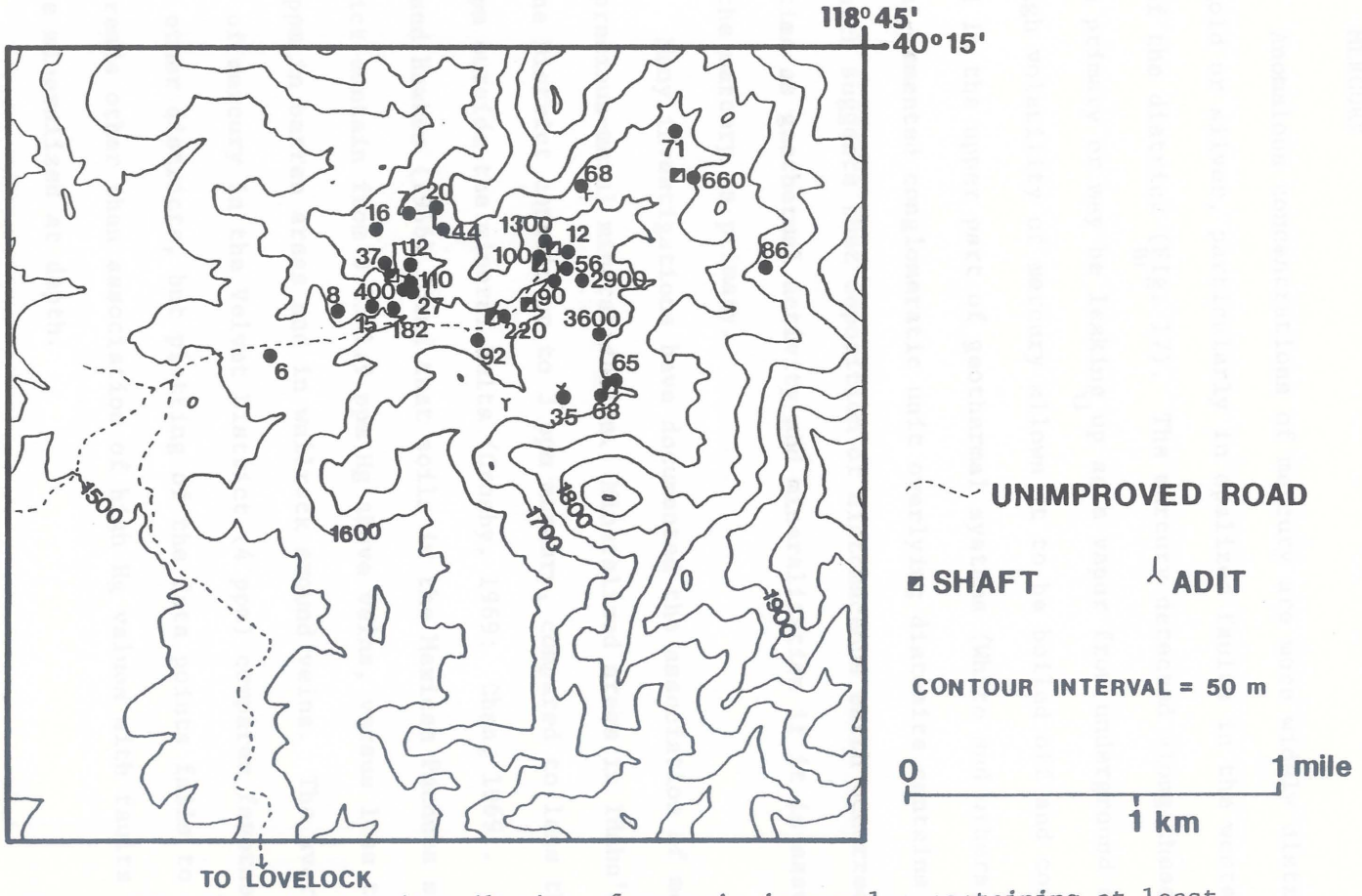

Figure 16. Map showing distribution of arsenic in samples containing at least 0.1 ppm gold. Values are ppm.

MERCURY

Anomalous concentrations of mercury are more widely distributed than gold or silver, particularly in opalized faults in the western part of the district (Fig. 17). The mercury detected along these faults may be primary or may be leaking up as a vapor from underground sources. The high volatility of mercury allows it to be boiled off and concentrated in the upper part of geothermal systems (White and others, 1971). An opal-cemented conglomeratic unit overlying diatomite contains 180 ppm Hg, which suggests that deposition of diatomaceous earth occurred at the same time as geothermal activity and mineralization if it is assumed that the mercury is primary.

Many investigations have documented the association of mercury with precious-metal mineralization. Mineralized areas in Idaho's Coeur d'Alene District contain up to 3 ppm mercury, compared to less than 0.5 ppm outside the mineral belts (Crosby, 1969; Chan, 1969). Friedrich and Hawkes (1966) found that soils in the Mexican Pachuca silver district contain from 0.25-1.9 ppm Hg above veins, versus less than 0.05 ppm in barren areas and in wallrock around veins. The average value of mercury in the Velvet District (4 ppm) compares favorably with these other districts, but plotting of the data points fails to reveal any trends other than association of high Hg values with faults which may be mineralized at depth.

LEAD

Lead was selected for analysis because Ashley and Albers (1975)

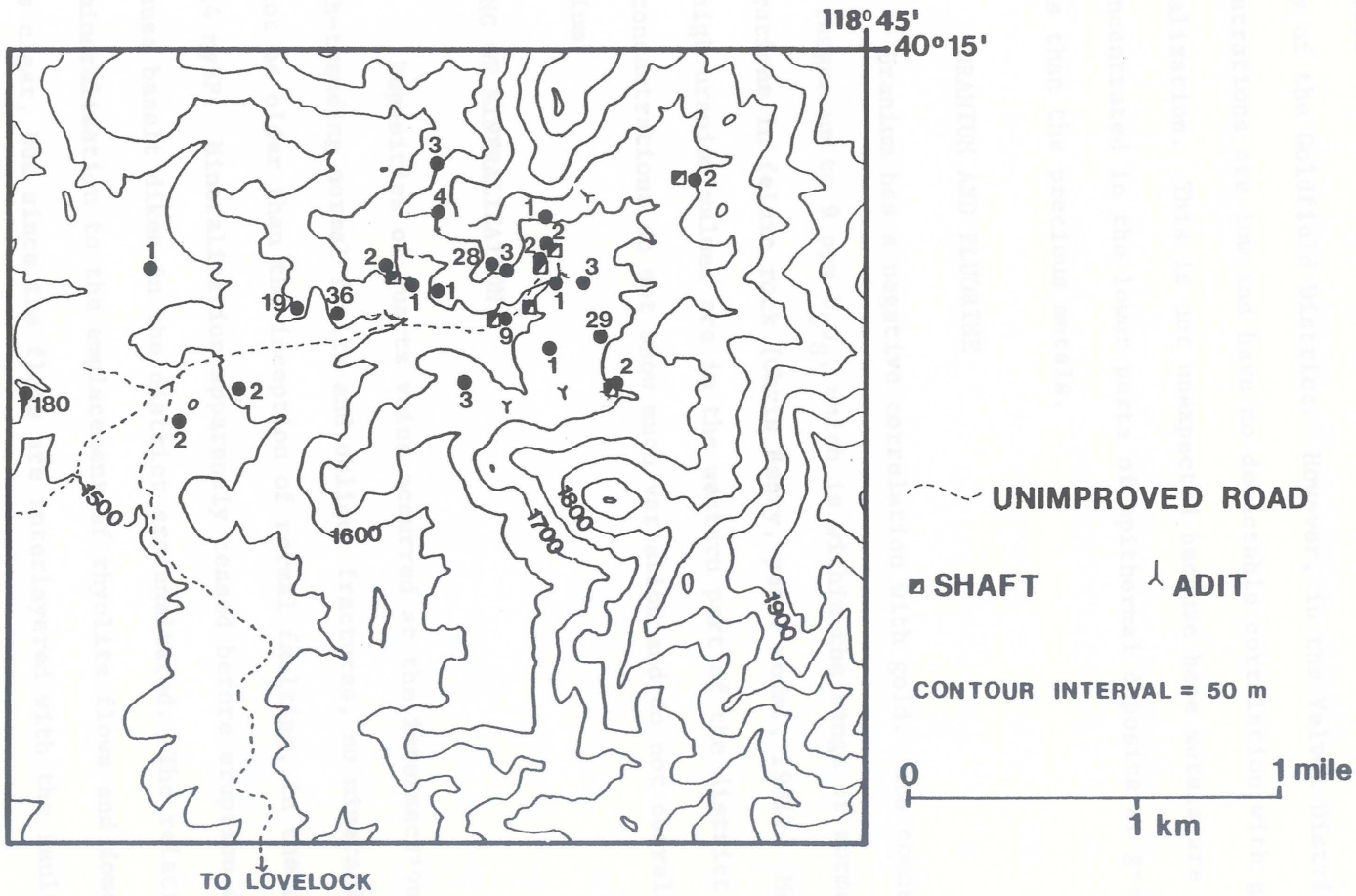

Figure 17. Map showing distribution of samples containing at least 1.0 ppm mercury. Values are ppm.

concluded that it would be the best gold indicator in a colluvial soil survey of the Goldfield District. However, in the Velvet District lead concentrations are low and have no detectable correlation with gold mineralization. This is not unexpected because base metals are commonly concentrated in the lower parts of epithermal deposits at greater depths than the precious metals.

URANIUM AND FLUORINE

Uranium has a negative correlation with gold. Its concentration ranges up to 9 ppm U_3O_8, which is within the range of normal concentrations in felsic rock (Chris Henry, pers. comm., 1981). Most of the high uranium values are in the western part of the district. Fluorine concentrations do not show much variation and do not correlate with uranium.

TIMING OF MINERALIZATION

Deposition of quartz veins occurred at the intersections of north-trending normal faults and oblique fractures, so mineralization cannot be older than the inception of normal faulting, in the time range 17-14 myBP. Mineralization apparently ceased before eruption of basalt because basalt dikes in the district are unaltered. The relationship of mineralization to the emplacement of rhyolite flows and domes is less clear, but since the flows are interlayered with the faulted tuffs it appears that they are not genetically related to mineralization. However, it is possible that some of the fresh rhyolites to the south and west of the district were erupted during the mineralization episode.

One small body of propylitically altered andesite outcrops near the center of the district, but its relationship to mineralization is unclear.

COMPARISON OF THE VELVET DISTRICT TO ACTIVE GEOTHERMAL SYSTEMS AND EPITHERMAL OREBODIES

WAIRAKEI AND BROADLANDS

The geothermal systems at Wairakei and Broadlands, New Zealand, are located in silicic volcanic rocks and interbedded lake deposits of Pliocene to Pleistocene age. Temperatures in the deeper parts of both areas average about 260° C and are nowhere hotter than 300° C. The alteration assemblage at Wairakei appears to be partially controlled by the vertical temperature gradient; montmorillonite is abundant only in the upper 300 m and mixed-layer clays extend downwards to depths of no more than 400 m (Fig. 18; Steiner, 1968). The alteration assemblages at Velvet do not fit this simple model, however, because some samples contain coexisting illite and smectite (sample 27; Table 2) and sample 78 contains only smectite despite fluid inclusion evidence that a quartz vein only centimeters away was deposited at 237 to 250° C, much hotter than the 160° C limit for smectite stability suggested by Steiner (1968). These troublesome relationships may be explained either by metastability or by circulation of hydrothermal waters through channels that were substantially hotter than the enclosing wallrock. If heat flow in the area was dominated by convection through fractures with very little conductive heat transfer, then the presence of smectites and mixed-layer clays implies regional temperatures less than 250° C. If it is assumed that subsurface temperature gradients in the district followed the hydrostatic boiling curve for pure water and that not more

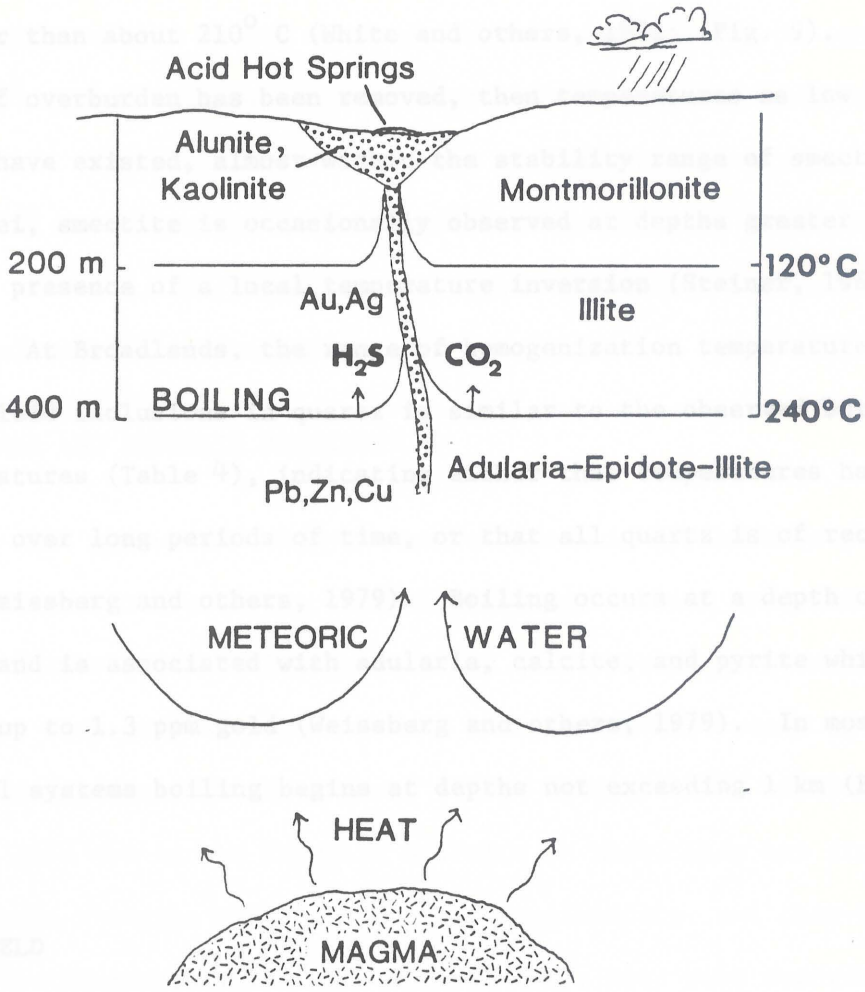

Figure 18. Schematic representation of the alteration zones in a geothermal system, modified from studies at Wairakei, New Zealand (Steiner, 1968).

than 200 m of overburden has been removed, than the ambient temperature at the level of exposure in the Velvet District should have been no greater than about 210° C (White and others, 1971; Fig. 9). If only 80 m of overburden has been removed, then temperatures as low as 170° C could have existed, almost within the stability range of smectite. At Wairakei, smectite is occasionally observed at depths greater than 300 m in the presence of a local temperature inversion (Steiner, 1968).

At Broadlands, the range of homogenization temperatures of primary fluid inclusions in quartz is similar to the observed borehole temperatures (Table 4), indicating either that temperatures have been stable over long periods of time, or that all quartz is of recent origin (Weissberg and others, 1979). Boiling occurs at a depth of 300-400 m and is associated with adularia, calcite, and pyrite which contains up to 1.3 ppm gold (Weissberg and others, 1979). In most geothermal systems boiling begins at depths not exceeding 1 km (Ellis, 1979).

GOLDFIELD

More than 4 million ounces of gold were recovered from Miocene volcanics immediately northeast of the town of Goldfield, Nevada (Ashley, 1974). Gold mineralization was localized in a 1 km^2 area of altered rock along a zone of ring fracturing. Hydrothermal alteration is zoned around the veins in the following sequence : (1) quartz, (2) illite-kaolinite, (3) montmorillonite, and (4) chlorite-calcite farthest from the vein (Harvey and Vitaliano, 1964). Alunite is present as a

supergene oxidation product in the veins and as a primary replacement of plagioclase phenocrysts (Jensen and others, 1971). Fluid inclusion data indicate that quartz was deposited at temperatures in the range 200-300° C, and boiling occurred over a 330 m vertical interval (Buchanan, 1981). Pyrophyllite, which forms at temperatures greater than 300° C, is present at Goldfield but has not been identified in the Velvet District, indicating either higher temperatures or a deeper level of erosion at Goldfield.

TUSCARORA AND REPUBLIC DISTRICTS

The gold-silver deposit at Tuscarora in northern Nevada is mentioned here because of the control lithology exerted upon mineralization. Silver lodes at Tuscarora occur in narrow veins in andesite, in contrast with gold ore which formed in wide fracture zones in bedded pyroclastics (Roberts and others, 1971; Nolan, 1936). Similarly, part of the gold ore in the Republic District in Washington was disseminated in altered volcanic breccia, volcanic conglomerate, and thin-bedded fine tuff (Worthington, 1981). The altered rocks have been described as

> white to cream colored and consist of light-colored silica in fine veinlets and chalky clay that has selectively replaced feldspar and some rock fragments...X-ray analysis of the clay...show it to be largely kaolinite...The flows beneath the sediments are bleached and consist predominantly of a porous chalky, somewhat crumbly mass of silica. This material constituted low-grade ore at the two mines... (Muessig, 1967).

The tuffs and sediments of the Velvet District may also host disseminated gold mineralization because they are pervasively fractured

and were not competent enough to support well-defined quartz veins. Surface mineralization is too diffuse to support mining at Velvet, but this may change at depth, especially if the tuffs acted as a cap to circulating geothermal fluids.

CONCLUSIONS

The fossil hydrothermal system exposed in the Velvet District has been shown to have the following characteristics:

1) Tuffs, flows, and coarse volcaniclastics suggest that the district was close to a Miocene volcanic center. The volcanics are cut by diffuse, poorly defined mineralized zones which may be good candidates for disseminated gold mineralization at depth;

2) Assays reveal significant amounts of pathfinder elements but subeconomic concentrations of gold and silver in surface outcrops;

3) The clay alteration assemblage suggests relatively low alteration temperatures, possibly within 200 m of the Tertiary paleosurface;

4) Fluid inclusions show evidence of boiling, but scarcity of adularia suggests that erosion has not yet exposed the deepest level of boiling in the system;

5) Hydrothermal fluids had temperatures of about 244° C and $\delta^{18}O$ of -13 °/oo prior to interaction with wallrock;

6) The patterns of alteration, ^{18}O, and temperatures of quartz veins delineate a small area in the southeast part of the district which appears to have been a major conduit of hydrothermal fluids. Areas of illite alteration are also

favorable places for subsurface exploration.

Future evaluation of the district should be concentrated in the southeast zone of low $\delta^{18}O$ veins and in the areas of illite-kaolinite alteration. The area of altered rock that extends outward to the west (Fig. 6) should also be explored further despite the high $\delta^{18}O$ of quartz because in some districts (e.g. Pachuca) productive veins die out upwards (Buchanan, 1981), and the quartz in the upper parts of these veins would be expected to become enriched in ^{18}O due to increased reaction with wallrock as the veins become constricted.

Identification of caldera collapse features or pervasive fault systems through detailed mapping of the volcanics in the Trinity Range is necessary to determine the overall structural setting of the Velvet District and to guide exploration outside its boundaries. Mapping of alteration outside the district will be hampered by cover of younger volcanics and Tertiary sediments, but the techniques described in this report should aid in the evaluation of isolated outcrops of quartz veins and argillic alteration.

Plate 1

Plates 1D-1F were photographed with crossed nicols.

A. View looking east showing the Trinity Range and the Velvet District. The white area is hydrothermally altered rhyolitic tuffs and flows. Basalt flows cap the range in the distance.

B. Ash-flow tuff. The dark lithic fragments are phyllite from the early Mesozoic Auld Lang Syne Formation which is not exposed in the district.

C. Ash-flow tuff with lithophysae. Flattened pumice fragments are visible in the pinkish matrix. The lithophysae have diameters of about 1 cm.

D. Tuffaceous sediment cemented by alunite. Scale bar is 1 mm.

E. Same sediment as 1D, but with higher magnification to show pore-filling alunite cement. Scale bar is 0.1 mm.

F. Quartz phenocryst in rhyolite flow with fluid inclusions. Scale bar is 0.1 mm.


A


B


C


D


E

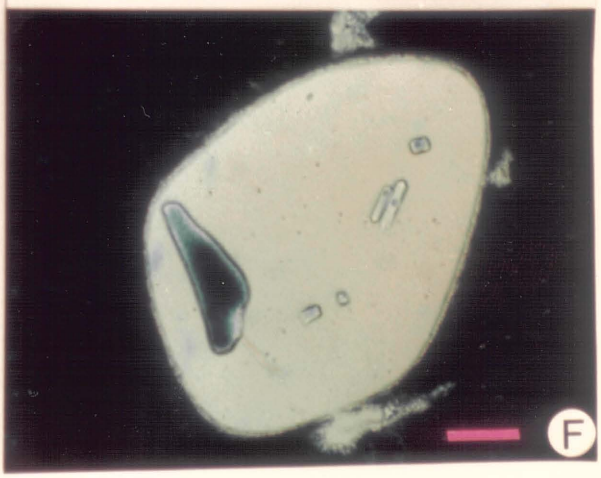
F

Plate 2

Plate 2E was photographed in plane polarized light. Plates 2B and 2C were photographed with crossed nicols.

A. View looking north showing the central part of the Velvet District. Several shafts and adits are located in the gully in the middle of the picture. North-northeast trending faults cut through the eastward-dipping tuff and tuffaceous sediment which forms the ridges in the center of the picture.

B. Ash-flow tuff. The bright white areas are flattened pumice fragments which have been replaced by quartz. Note the zoned alkali feldspar crystal in the upper left. Scale bar is 1 mm.

C. Spherulitic ash-flow tuff. Tridymite lines the cores of the hollow spherulites in the center and top of the picture. Granophyric quartz-alkali feldspar intergrowths are visible on the left side of the picture and just above the C on the lower right. Scale bar is 0.5 mm.

D. Large recumbent fold formed during slumping of thick intracaldera (?) ash-flow tuff. The nose of the fold is to the right, and the axial plane is approximately horizontal from left to right across the photo.

E. Flow banding in spherulitic rock. The origin of this sample is debatable, but the absence of shards and exotic fragments suggest that it is a lava flow. Scale bar is 5 mm.


A


B


D

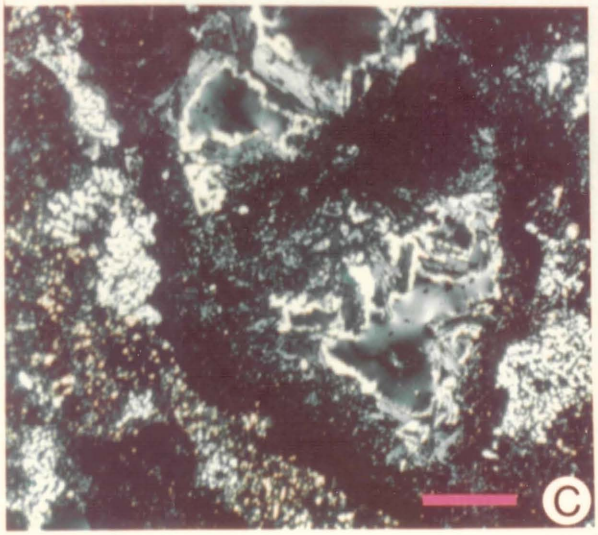
C


E

Plate 3

Plate 3A was photographed in plane polarized light.
Plates 3D-3F were photographed with crossed nicols.

A. Alkali feldspar phenocrysts in a green vitrophyre at the base of an ash-flow tuff. Outlines of shards are evident in the area between the two phenocrysts but are not preserved in the remainder of the groundmass. The phenocrysts are concentrically zoned, and are fractured and partially altered to kaolinite and calcite. Scale bar is 0.5 mm.

B. SEM photomicrograph of diatomaceous earth from a prospect pit below the base of a basalt flow. The diatom species is Melosira granulata. Scale bar is 2 microns.

C. View looking north showing westward-dipping basalt flows downfaulted against light colored tuffs. The lower basalt flow, dipping at about 30 degrees, was faulted and tilted prior to extrusion of the more shallowly dipping upper basalt flow. Bright white patches on the extreme left below the flows are diatomite.

D. Skeleton olivine phenocryst in basalt. Incipient alteration to iddingsite is visible along fractures in the crystal. Scale bar is 1 mm.

E. Hydrothermal alteration in sample 94. The feldspar crystal has been completely altered to illite and quartz. The rectangular outline of the feldspar crystal is preserved in the silicified groundmass. Scale bar is 0.5 mm.

F. Hydrothermal alteration in sample 20. The feldspar crystal has been altered to a mixed-layer illite/smectite which has optical properties similar to smectite. The groundmass is silicified and contains small amounts of limonite and kaolinite. Scale bar is 0.5 mm.

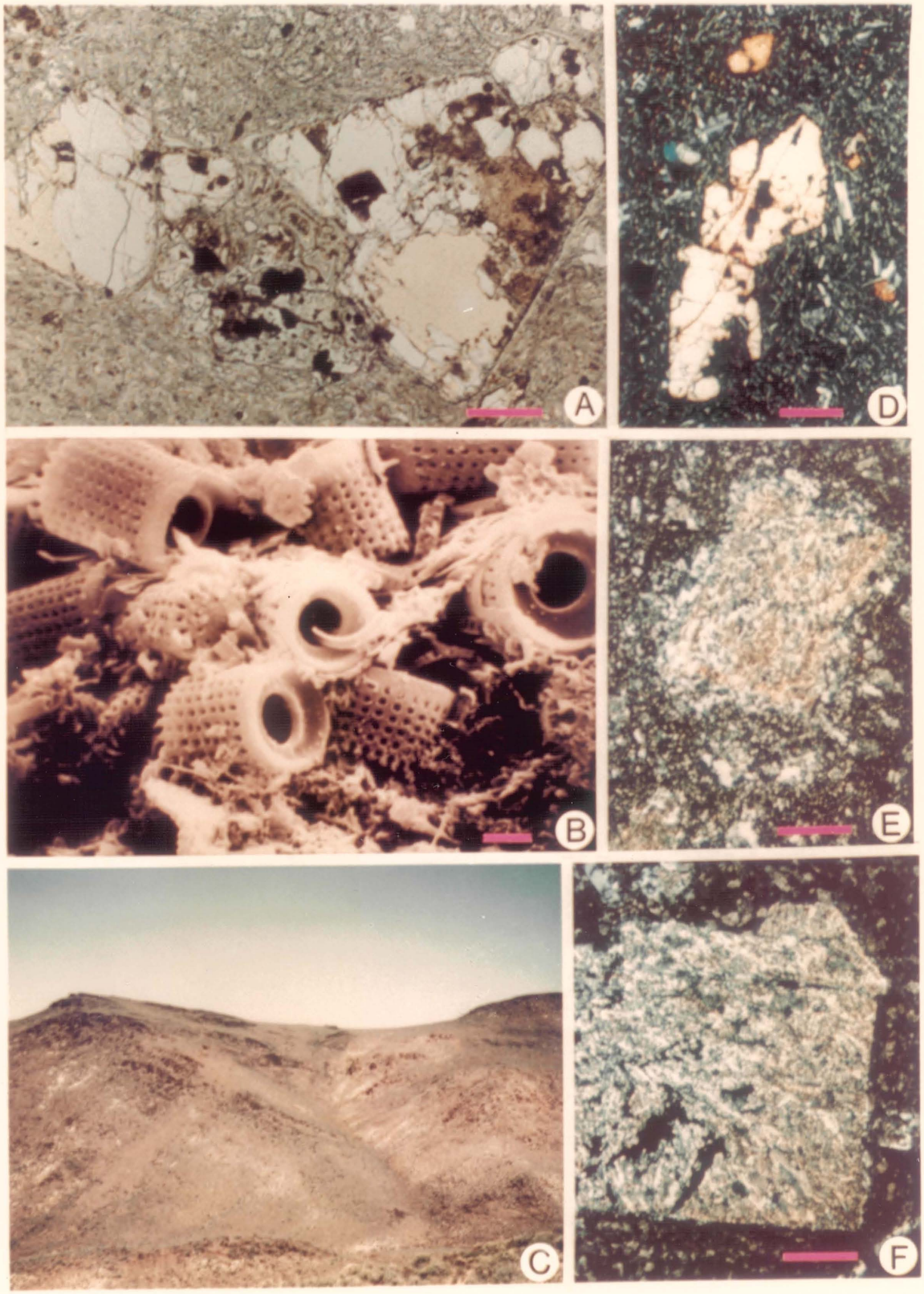
A
D
B
E
C
F

Plate 4

Plates 4B and 4E were photographed in plane polarized light. Plate 4F was photographed with crossed nicols.

A. Small adit into bleached outcrop of massive clay. X-ray diffraction analysis shows that the hydrothermal clay is mixed-layer illite/smectite. Sample 20 from this outcrop contained 0.4 ppm Au.

B. Altered feldspar in sample 19. Spheres of limonite are concentrated around the margin of the altered crystal and are also scattered throughout the groundmass. Scale bar is 0.1 mm.

C. Quartz veinlet in sample 90. The milky quartz veinlet visible just above the scale bar postdates the dark areas of brecciation and argillic alteration. A sample of this rock assayed 0.3 ppm Au.

D. Quartz vein in sample 26. The scale bar is on silicified, brecciated tuff. Three generations of quartz are visible in the vein on the upper half of the sample. Vein and wallrock of this sample contain 0.1 ppm Au.

E. Photomicrograph of the vein shown in 4D above. Altered adularia ("A") is intergrown with quartz. Scale bar is 0.5 mm.

F. Feathered quartz grain, also from sample 26. Direction of vein growth was towards the top of the photomicrograph. Salt and pepper chalcedony overgrowths are visible on the sides and top of the feathered quartz. Scale bar is 0.1 mm.


A


cm
D

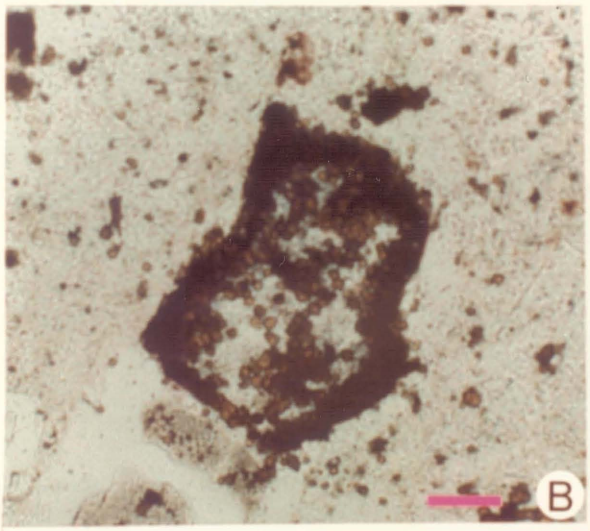
B

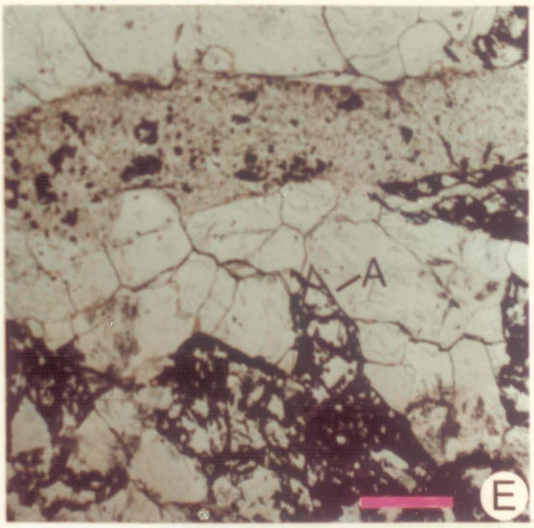
A
E

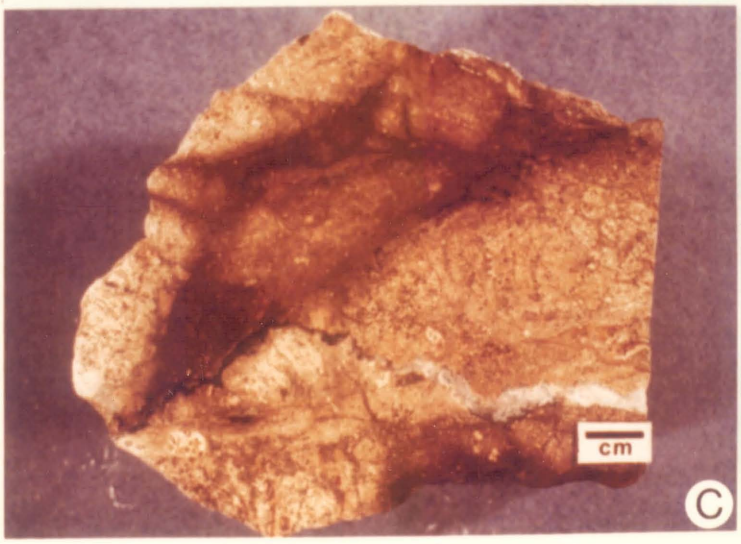
cm
C


F

Plate 5

Plates 5A-5C were photographed in plane polarized light.

A. Fluid inclusions in a single quartz crystal from sample 33. The elongate inclusions are primary. The inclusion in the upper right hand corner is secondary. Scale bar is 0.025 mm.

B. Large primary inclusion in a single quartz crystal from sample 94. Unfortunately, this inclusion leaked during heating. Scale bar is 0.05 mm.

C. Empty fluid inclusions in a single quartz crystal from sample 33. The four negative crystals in the lower half of the picture are empty or only slightly wet by fluids. A secondary inclusion with bubble is visible in the upper left corner. Scale bar is 0.1 mm.

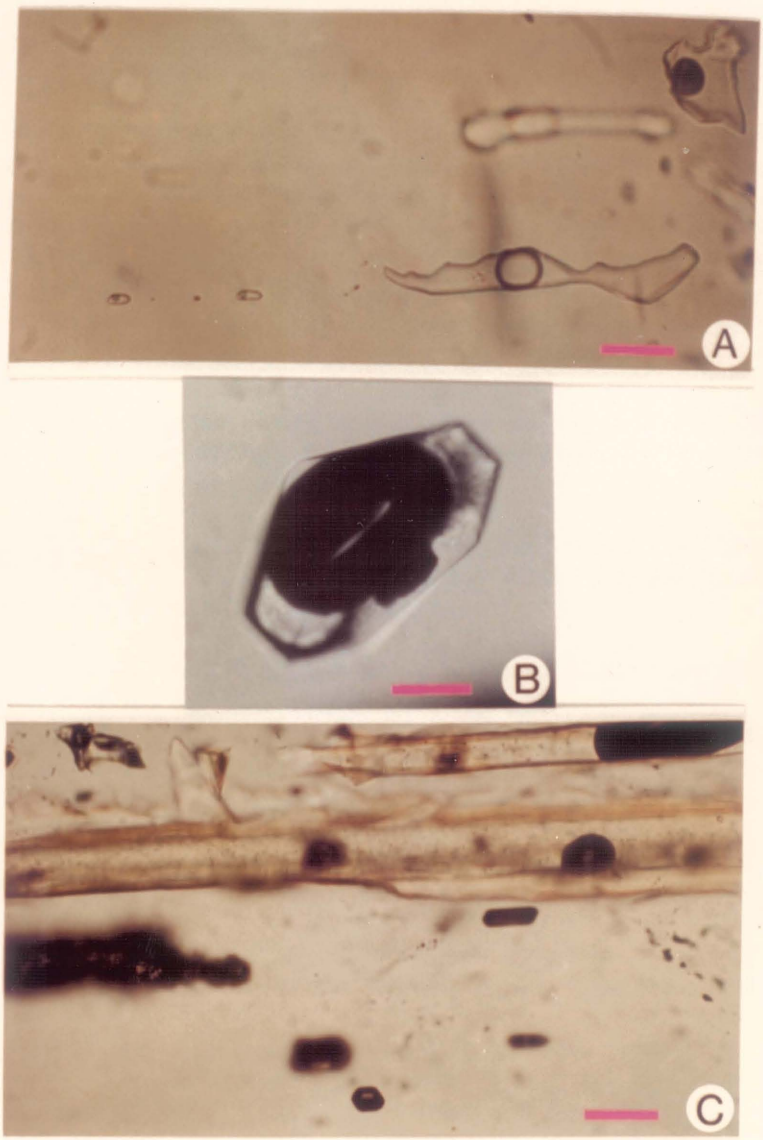
A
B
C

REFERENCES

Adams, Sidney F., 1920, A microscopic study of vein quartz: Econ. Geol., v. 15, pp. 623-664.

Akright, Robert L., Radtke, Arthur S., and Grimes, David J., 1969, Minor elements as guides to gold in the Roberts Mountains Formation, Carlin gold mine, Eureka County, Nevada, in Canney, F.C., ed., International geochemical exploration symposium: Colorado School Mines Quart., v. 64, no. 1, pp. 49-66.

Ashley, Roger P., 1974, Goldfield mining district, in Guidebook to the geology of four Tertiary volcanic centers in central Nevada: Nev. Bur. Mines Rep. 19, pp. 49-66.

Ashley, R.P., and Albers, J.P., 1975, Distribution of gold and other ore-related elements near ore bodies in the oxidized zone at Goldfield, Nevada: U.S. Geol. Survey Prof. Paper 843-A, pp. A1-A48.

Barnes, Hubert Lloyd, 1979, Solubilities of ore minerals, in Barnes, H.L., ed., Geochemistry of Hydrothermal Ore Deposits, 2nd ed.: New York, John Wiley and Sons, pp. 404-454.

Bayliss, P., Loughnan, F.C., and Standard, J.C., 1965, Dickite in the Hawkesbury sandstone of the Sydney basin, Australia: Am. Mineralogist, v. 50, pp. 418-426.

Browne, P.R.L., and Ellis, A.J., 1970, The Ohaki-Broadlands hydrothermal area, New Zealand: Mineralogy and related geochemistry: Am. Jour. Sci., v. 269, pp. 97-131.

Buchanan, L.J., 1981, Precious metal deposits associated with volcanic environments in the southwest, in Dickinson, W.R., and Payne, W.D., eds., Relations of tectonics to ore deposits in the southern Cordillera: Arizona Geological Society Digest, v. 24, pp. 237-262.

Burritt, A.G., 1919, Unpublished report for Gold Note Mining Co., 5 pp.

Carroll, Dorothy, 1970, Clay Minerals: a guide to their X-ray identification: Geol. Soc. Am. Spec. Paper 126, pp. 1-80.

Chan, Samuel S.M., 1969, Suggested guides for exploration from geochemical investigation of ore veins at the Galena Mine deposits, Shoshone County, Idaho, in Canney, F.C., ed., International geochemical exploration symposium: Colorado School Mines Quart.,

v. 64, no. 1, pp. 139-168.

Christiansen, Robert L., and McKee, Edwin H., 1978, Late Cenozoic volcanic and tectonic evolution of the Great Basin and Columbia Intermontane regions, in Smith, R.B., and Eaton, G.P., eds., Cenozoic tectonics and regional geophysics of the western Cordillera: Geol. Soc. America Mem. 152, pp. 283-311.

Clayton, R.N., and Mayeda, T.K., 1963, The use of bromine pentafluoride in the extraction of oxygen from oxides and silicates for isotopic analysis: Geochim. et Cosmochim. Acta, v. 27, pp. 43-52.

Clayton, T.N., and Steiner, A., 1975, Oxygen isotope studies of the geothermal system at Wairakei, New Zealand: Geochim. et Cosmochim. Acta, v. 39, pp. 1179-1186.

Craig, H., 1961, Isotopic variations in meteoric waters: Sciences, v. 133, pp. 1702-1703.

Craig, H., 1963, The isotopic geochemistry of water and carbon in geothermal areas, in Tongiorgi, E., ed., Nuclear geology of geothermal areas: Consiglio Nazionale delle Ricerche Laboratoria de geologia nucleara, Pisa, pp. 17-53.

Crosby, G.M., 1969, A preliminary examination of trace mercury in rocks, Coeur d'Alene district, Idaho, in Canney, F.C., ed., International geochemical exploration symposium: Colorado School Mines Quart., v. 64, no. 1, pp. 169-194.

Ellis, A.J., 1970, Quantitative interpretation of chemical characteristics of hydrothermal systems: Geothermics, special issue 2, pp. 516-528.

Ellis, A.J., 1979, Explored geothermal systems, in Barnes, H.L., ed., Geochemistry of Hydrothermal Ore Deposits, 2nd ed.: New York, John Wiley and Sons, pp. 632-683.

Eslinger, E.V., and Savin, S.M., 1973, Mineralogy and oxygen isotope geochemistry of the hydrothermally altered rocks of the Ohaki-Broadlands, New Zealand geothermal area: Am. Jour. Sci., v. 273, pp. 240-267.

Field, C.W., and Lombardi, G., 1972, Sulfur isotopic evidence for the supergene origin of alunite deposits, Tolfa District, Italy: Mineral. Deposita, v. 7, pp. 113-125.

Friedman, I., and O'Neil, J.R., 1977, Data of Geochemistry, sixth edition, Chapter KK: Compilation of stable isotope fractionation factors of geochemical interest: U.S. Geol. Survey Prof. Paper 440-KK.

Friedrich, G.H., and Hawkes, H.E., 1966, Mercury as an ore guide in the Pachuca-Real del Monte District, Hildalgo, Mexico: Econ. Geol., v. 61, pp. 744-753.

Goldschmidt, V.M., 1954, Geochemistry: Oxford, Clarendon Press, 730 pp.

Hamilton, Warren, 1969, The volcanic central Andes - a modern model for the Cretaceous batholiths and tectonics of western North America, in McBirney, A.R., ed., Proceedings of the Andesite Conference: Oregon Dept. of Geology and Mineral Industries, Bull. 65, pp. 175-184.

Harvey, Richard D., and Vitaliano, Charles J., 1964, Wall-rock alteration in the Goldfield district, Nevada: Jour. Geology, v. 72, pp. 564-579.

Hemley, J.J., Hostetler, P.B., Gude, A.J., and Mountjoy, W.T., 1969, Some stability relations of alunite: Econ. Geol., v. 64, pp. 599-612.

Jenson, M.L., Ashley, T.P., and Albers, J.P., 1971, Primary and secondary sulfates at Goldfield, Nevada: Econ. Geol., v. 66, pp. 618-626.

Johnson, Maureen G., 1977, Geology and mineral deposits of Pershing County, Nevada: Nevada Bur. Mines and Geology Bull. 89, 115 pp.

Kerr, Paul F., 1977, Optical Mineralogy: New York, McGraw-Hill Book Company, 492 pp.

Krauskopf, K.B., 1967, Introduction to geochemistry: New York, McGraw-Hill Book Co., 721 pp.

Leeman, William P., and Rogers, John J.W., 1970, Late Cenozoic alkali-olivine basalts of the Basin-Range Province, USA: Cont. Mineral. and Petrol., v. 25, pp. 1-24.

Lindgren, W., 1928, Mineral Deposits, 3rd ed.: New York, McGraw-Hill Book Co., 1049 pp.

McKee, E.H., and Marvin, R.M., 1973, Summary of radiometric ages of Tertiary volcanic rocks in Nevada. Part IV, Northwestern Nevada: Isochron/West, no. 10, pp. 1-7.

Muessig, Siegfried, 1967, Geology of the Republic quadrangle and a part of the Aneas quadrangle, Ferry County, Washington: U.S. Geol. Survey Bull. 1216, 135 pp.

Nash, J. Thomas, 1972, Fluid inclusion studies of some gold deposits in Nevada: U.S. Geol. Survey Prof. Paper 800-C, pp. C15-C19.

Nolan, T.B., 1936, The Tuscarora mining district, Nevada: Univ. Nev. Bull., v. 30, 38 pp.

O'Neil, J.R., Silberman, M.L., Fabbi, B.P., and Chesterman, C.W., 1973, Stable isotope and chemical relations during mineralization in the Bodie mining district, Mono County, California: Econ. Geol., v. 68, pp. 765-784.

O'Neil, J.R., and Silberman, M.L., 1974, Stable isotope relations in epithermal Au-Ag deposits: Econ. Geol., v. 69, pp. 902-909.

Roberts, Ralph J., Radtke, Arthur S., and Coats, R.R., 1971, Gold-bearing deposits in north-central Nevada and southwestern Idaho: Econ. Geol., v. 66, pp. 14-33.

Roedder, Edwin, 1970, Application of an improved crushing microscope stage to studies of the gases in fluid inclusions: Schweiz. Min. Petr. Mitt., v. 50, Pt. 1, pp. 41-58.

Roedder, Edwin, 1976, Fluid inclusion evidence on the genesis of ores in sedimentary and volcanic rocks, in Wolf, K.H., ed., Handbook of Strata-bound and Stratiform Ore Deposits, v. 2: Elsevier, Amsterdam, pp. 67-110.

Roedder, Edwin, 1979, Fluid inclusions as samples of ore fluids, in Barnes, H.L., ed., Geochemistry of Hydrothermal Ore Deposits, 2nd ed.: New York, John Wiley and Sons, pp. 684-737.

Rose, Arthur W., and Burt, Donald M., 1979, Hydrothermal alteration, in Barnes, H.L., ed., Geochemistry of Hydrothermal Ore Deposits, 2nd ed.: New York, John Wiley and Sons, pp. 173-235.

Schoen, Robert, White, Donald E., and Hemley, J.J., 1974, Argillization by descending acid at Steamboat Springs, Nevada: Clays and Clay Minerals, v. 22, pp. 1-22.

Smith, H.G., McKee, E.H., Tatlock, D.B., and Marvin, R.F., 1971, Mesozoic granitic rocks in northwestern Nevada - a link between the Sierra Nevada and Idaho Batholiths: Geol. Soc. America Bull., v. 82, pp. 2933-2944.

Spurr, Josiah Edward, 1905, Geology of the Tonopah mining district, Nevada: U.S. Geol. Survey Prof. Paper 42, pp. 1-295.

Steiner, A., 1968, Clay minerals in hydrothermally altered rocks at Wairakei, New Zealand: Clays and Clay Minerals, v. 16, pp. 193-213.

Taylor, Hugh P., Jr., 1968, The oxygen isotope geochemistry of igneous rocks: Contr. Mineral. and Petrol., v. 19, pp. 1-71.

Taylor, Hugh P., Jr., 1973, O^{18}/O^{16} evidence for meteoric-hydrothermal alteration and ore deposition in the Tonopah, Comstock Lode, and Goldfield mining districts, Nevada: Econ. Geol., v. 68, pp. 747-764.

Taylor, Hugh P., Jr., 1974, The application of oxygen and hydrogen isotope studies to problems of hydrothermal alteration and ore deposition: Econ. Geol., v. 69, pp. 843-883.

Vanderburg, W.D., 1936, Reconnaissance of mining districts in Pershing County, Nevada: U.S. Bur. Mines Inf. Circ. 6902.

Weissberg, B.G., 1969, Gold-silver ore-grade precipitates from New Zealand thermal waters: Econ. Geol., v. 64, pp. 95-108.

Weissberg, Byron G., Browne, Patrick R.L., and Seward, Terry M., 1979, Ore metals in active geothermal systems, in Barnes, H.L., ed., Geochemistry of Hydrothermal Ore Deposits, 2nd ed.: New York, John Wiley and Sons, pp. 738-780.

White, Donald E., Brannock, W.W., and Murata, K.J., 1956, Silica in hot-spring waters: Geochim. et Cosmochim. Acta, v. 10, pp. 27-59.

White, D.E., 1967, Mercury and base-metal deposits with associated thermal and mineral waters, in Barnes, H.L., ed., Geochemistry of Hydrothermal Ore Deposits, 1st ed.: New York, Holt, Rinehart and Winston, pp. 575-631.

White, D.E., Muffler, L.J.P., and Truesdell, A.H., 1971, Vapor-dominated hydrothermal systems compared with hot-water systems: Eonc. Geol., v. 66, pp. 75-97.

Willden, Ronald, and Speed, R.C., 1974, The geology and mineral deposits of Churchill County, Nevada: Nevada Bur. Mines and Geology Bull. 83, 95 pp.

Worthington, Joseph E., 1981, Bulk tonnage gold deposits in volcanic environments, in Dickinson, W.R., and Payne, W.D., eds., Relations of tectonics to ore deposits in the southern Cordillera: Arizona Geological Society Digest, v. 24, pp. 263-270.

VITA

Wilmer Dallam Masterson IV, the son of Dorothy and Bill Masterson, was born in Dallas, Texas, on July 4, 1957. He graduated from Highland Park High School, Dallas, in 1975 and entered Yale University. The summers of 1977 and 1978 were spent exploring for geothermal resources in Nevada. After receiving a B.S. from Yale in 1979 he began graduate studies at The University of Texas at Austin in September, 1979.

Permanent address: 3812 Stratford
Dallas, Texas 75202

This thesis was typed by Donna L. Precht.